PLOS ONE

Differential coexistence of multiple genotypes of *Ophiocordyceps sinensis* in the stromata, ascocarps and ascospores of natural *Cordyceps sinensis*

Yu-Ling Li[1¶], Xiu-Zhang Li[1¶], Yi-Sang Yao[2¶], Zi-Mei Wu[3], Ling Gao[2], Ning-Zhi Tan[2], Zhou-Qing Luo[3,#a], Wei-Dong Xie[2], Jian-Yong Wu[4,5], Jia-Shi Zhu[1,2]*

[1] State Key Laboratory of Plateau Ecology and Agriculture, Qinghai Academy of Animal and Veterinary Sciences, Qinghai University, Xining, Qinghai, China

[2] Shenzhen Key Laboratory of Health Science and Technology, Institute of Biopharmaceutical and Health Engineering, Shenzhen International Graduate School, Tsinghua University, Shenzhen 518055, China

[3] School of Life Sciences, Tsinghua University, Beijing, China

[4] State Key Laboratory of Chinese Medicine and Molecular Pharmacology, Shenzhen 518057, Guangdong, China

[5] Department of Applied Biology and Chemistry Technology, The Hong Kong Polytechnic University, Hong Kong

[#a] Current address: State Key Laboratory of Cellular Stress Biology, School of Life Sciences, Faculty of Medicine and Life Sciences, Xiamen University, Xiamen 361102, China

* Corresponding author

E-mail: zhujosh@163.com (JSZ)

[¶] These authors contributed equally to this work.

Short title:

Differential occurrence of *Ophiocordyceps sinensis* genotypes in natural *Cordyceps sinensis*

Abstract

Objective: To examine the differential occurrence of *Ophiocordyceps sinensis* genotypes in the stroma, stromal fertile portion (SFP) densely covered with numerous ascocarps, and ascospores of natural *Cordyceps sinensis*. **Methods:** Immature and mature *C. sinensis* specimens were harvested. Mature *C. sinensis* specimens were continuously cultivated in our laboratory (altitude 2,200 m). The SFPs (with ascocarps) and ascospores of *C. sinensis* were collected for microscopic and molecular analyses using species-/genotype-specific primers. Sequences of mutant genotypes of *O. sinensis* were aligned with that of Genotype #1 *Hirsutella sinensis* and compared phylogenetically using a Bayesian majority-rule method. **Results:** Fully and semiejected ascospores were collected from the same specimens. The semiejected ascospores tightly adhered to the surface of the asci as observed by the naked eye and under optical and confocal microscopies. The multicellular heterokaryotic ascospores showed uneven staining of nuclei. The immature and mature stromata, SFPs (with ascocarps) and ascospores were found to differentially contain several GC- and AT-biased genotypes of *O. sinensis*, *Samsoniella hepiali*, and an AB067719-type fungus. The genotypes within AT-biased Cluster-A in the Bayesian tree occurred in all compartments of *C. sinensis*, but those within AT-biased Cluster-B were present in immature and mature stromata and SPFs but absent in the ascospores. Genotype #13 of *O. sinensis* was present in semi-ejected ascospores and Genotype #14 in fully ejected ascospores. GC-biased Genotypes #13–14 featured large DNA segment substitutions and genetic material recombination between the genomes of the parental fungi (*H. sinensis* and the AB067719-type fungus). These ascosporic offspring genotypes combined with varying abundances of *S. hepiali* in the 2 types of ascospores participated in the control of the development, maturation and ejection of the ascospores. **Conclusion:** Multiple genotypes of *O. sinensis* coexist differentially in the stromata, SFPs and 2 types of *C. sinensis* ascospores, along with *S. hepiali* and the AB067719-type fungus. The fungal components in different combinations and their dynamic alterations in the compartments of *C. sinensis* during maturation play symbiotic roles in the lifecycle of natural *C. sinensis*.

Keywords: natural *Cordyceps sinensis*; ascospores; stromal fertile portion (densely covered with numerous ascocarps); mutant genotypes of *Ophiocordyceps sinensis*; *Hirsutella sinensis* (Genotype #1 of *O. sinensis*); multicellular heterokaryon; *Samsoniella hepiali* (synonym *Paecilomyces hepiali*); AB067719-type fungus

Introduction

Natural *Cordyceps sinensis* is one of the most highly valued therapeutic agents in traditional Chinese medicine (TCM) and has been used for centuries in clinics as a folk medicine for "Yin-Yang" double invigoration, health maintenance, disease amelioration, and post-disease/surgery recovery [1–2]. Modern pharmacological studies have validated the therapeutic profile and lifespan-extending properties of natural *C. sinensis* and its mycelial fermentation products [2–6]. The Chinese Pharmacopeia defines natural *C. sinensis* as an insect-fungal complex consisting of the fruiting body of *Ophiocordyceps sinensis* and the remains of Hepialidae moth larva, *i.e.*, natural *C. sinensis* ≠ *O. sinensis* fungus [7–12]. Studies have reported that the caterpillar body of *C. sinensis* contains an intact larval intestine, an intact and thick larval body wall with numerous bristles, head tissues, and fragments of other larval tissues [8–12]. The controversy surrounding the indiscriminate use of Latin names (*Cordyceps sinensis* and *Ophiocordyceps sinensis* since 2007) for the natural insect-fungal complex and multiple anamorphic-teleomorphic fungi has been addressed both in Chinese and English [7–12]. In this paper, we temporarily refer to the fungus/fungi as *O. sinensis* and continue the customary use of the name *C. sinensis* for the wild or cultivated insect-fungal complex, although this practice will likely be replaced by the discriminative use of exclusive Latin names in the future.

Natural *C. sinensis* grows only in alpine areas at altitudes above 3,000–3,500 m on the Qinghai-Tibetan Plateau and has a complex lifecycle [2,12–14]. Its maturation stages, which have been used as a market standard for grading the quality of natural *C. sinensis*, greatly impact its mycobiota profile, metagenomic polymorphism, metatranscriptomic and proteomic expression, chemical constituent fingerprint, competitive proliferation of *Hirsutella sinensis*-like fungi, and therapeutic efficacy and potency as a natural therapeutic agent [7–10,12,14–28]. Mycologists have identified 22 species from 13 fungal genera in this insect-fungal complex [29], and culture-independent molecular methodologies have identified >90 fungal species spanning more than 37 genera and 12 genotypes of *O. sinensis* and demonstrated the predominance of different fungi and metagenomic fungal diversity in the stroma and caterpillar body of natural and cultivated *C. sinensis* [9,15–16,18,24,27–29,32–42].

Wei et al. [44] hypothesized that *H. sinensis* is the sole anamorph of *O. sinensis*. This hypothesis was primarily based on 3 lines of evidence: (1) frequent isolation and mycological identification according to sporulation, conidial morphology and growth characteristics [29]; (2) the microcycle conidiation of

ascospores [45–47]; and (3) systematic molecular analyses *via* internal transcribed spacer (ITS) sequencing and random molecular marker polymorphism assays [25,33–37,44,48–49]. Wei et al. [50] reported an industrial artificial cultivation project and demonstrated a mismatch between the inoculants of 3 GC-biased Genotype #1 *H. sinensis* strains and a sole teleomorphic fungus (AT-biased Genotype #4 of *O. sinensis*) in the fruiting body of cultivated *C. sinensis*. The sequences of the AT-biased genotypes of *O. sinensis* are absent in the genome of GC-biased Genotype #1 *H. sinensis* and belong to independent *O. sinensis* fungi [7–12,24,30–31,43,51–56]. Thus, according to the fourth criterion of Koch's postulates, the species contradiction between the anamorphic inoculants and the teleomorph in cultivated products disproves the sole anamorph hypothesis for *H. sinensis* that was proposed by Wei et al. [44] of the same research group 10 years ago. The teleomorphs of *O. sinensis* found in natural *C. sinensis* specimens collected from geographically distant areas and cultivated *C. sinensis* reportedly belong to Genotypes #1, #2, #3, #4, #5 or #7 [27–28,32–37,44,48–49,57–60], whereas those found in ascospores of *C. sinensis* reportedly belong to both GC-biased Genotype #1 and AT-biased Genotype #5 of *O. sinensis* fungi [61]. In addition to the report of species contradiction between the anamorphic inoculants (GC-biased Genotype #1) and teleomorphs (AT-biased Genotype #4) in cultivated *C. sinensis*, Wei et al. [50] identified teleomorphic Genotype #1 of *O. sinensis* in natural *C. sinensis*. Because the majority of the fungal species present in the natural world are most likely nonculturable [62–64], culture-independent molecular approaches have been widely used, resulting in the identification of 12 genotypes of *O. sinensis* and many other fungi from natural and cultivated *C. sinensis* in previous studies [9,16-18,24,27–28,30–37,48,50,56–61,65–67].

In this study, natural *C. sinensis* specimens were collected from the Hualong and Yushu areas of Qinghai Province and cultivated continuously in our laboratory in Xining city (altitude of 2,200 m). The histology of the stromal fertile portion (SFP) that was densely covered with ascocarps and ascospores of *C. sinensis* was examined under optical, confocal and fluorescence microscopes. Multiple genotypes of *O. sinensis* and other *C. sinensis*-associated fungi were profiled in the immature and mature stromata, fertile portion of the mature stroma and 2 types of ascospores of natural *C. sinensis* using species- and genotype-specific PCR primers, amplicon sequencing and cloning-based sequencing approaches.

Materials and Methods

132 ## Reagents

133 Laboratory common reagents such as ethanol, sucrose, paraformaldehyde, hematoxylin, eosin,
134 agarose and electrophoresis reagents, etc. were purchased from Beijing Bioland Technology Company.
135 Mercuric chloride (0.1%) for surface sterilization of freshly collected *C. sinensis* specimens was a gift
136 from the Institute of Microbiology, Chinese Academy of Sciences. *Eco*RI endonuclease is a product of
137 New England BioLabs, United States. The Universal DNA Purification kit was a product of TIANGEN
138 BIOTECH Company, China. The DNeasy Plant Mini Kit was a product of Qiagen Company, Germany.
139 The Gel Extraction Kit was a product of Omega Bio-Tek, United States. The *Taq* PCR reagent kit and
140 Vector NTI Advance 9 software were purchased from Invitrogen, United States. Calmodulin was a product
141 of Abicom (Shanghai, China).

142

143 ## Collection of *C. sinensis* specimens and ascospores

144 Immature *C. sinensis* specimens were purchased from local markets from the Hualong (located at
145 36°13'N, 102°19'E) and Yushu areas (located at 33°01'N, 96°48'E) of Qinghai Province of China (3800–
146 4600 m' altitude) in mid-May and characterized by a plump caterpillar body and very short stroma (1.0–
147 2.0 cm) [19,27]. Mature *C. sinensis* specimens were collected in mid-June and characterized by a plump
148 caterpillar body and long stroma (>5.0 cm) and by the formation of an expanded fertile portion close to
149 the stromal tip, which was densely covered with ascocarps (Fig 1). Governmental permission was not
150 required for *C. sinensis* purchases in local markets, and the collections of *C. sinensis* specimens from sales
151 by local farmers fall under the governmental regulations for traditional Chinese herbal products.

152 The specimens were washed thoroughly on site in running water with gentle brushing, soaked in
153 0.1% mercuric chloride for 10 min for surface sterilization and washed 3 times with sterile water. The
154 thoroughly cleaned specimens were immediately frozen in liquid nitrogen on site and kept frozen during
155 transportation to the laboratory and during storage prior to further processing [19,27].

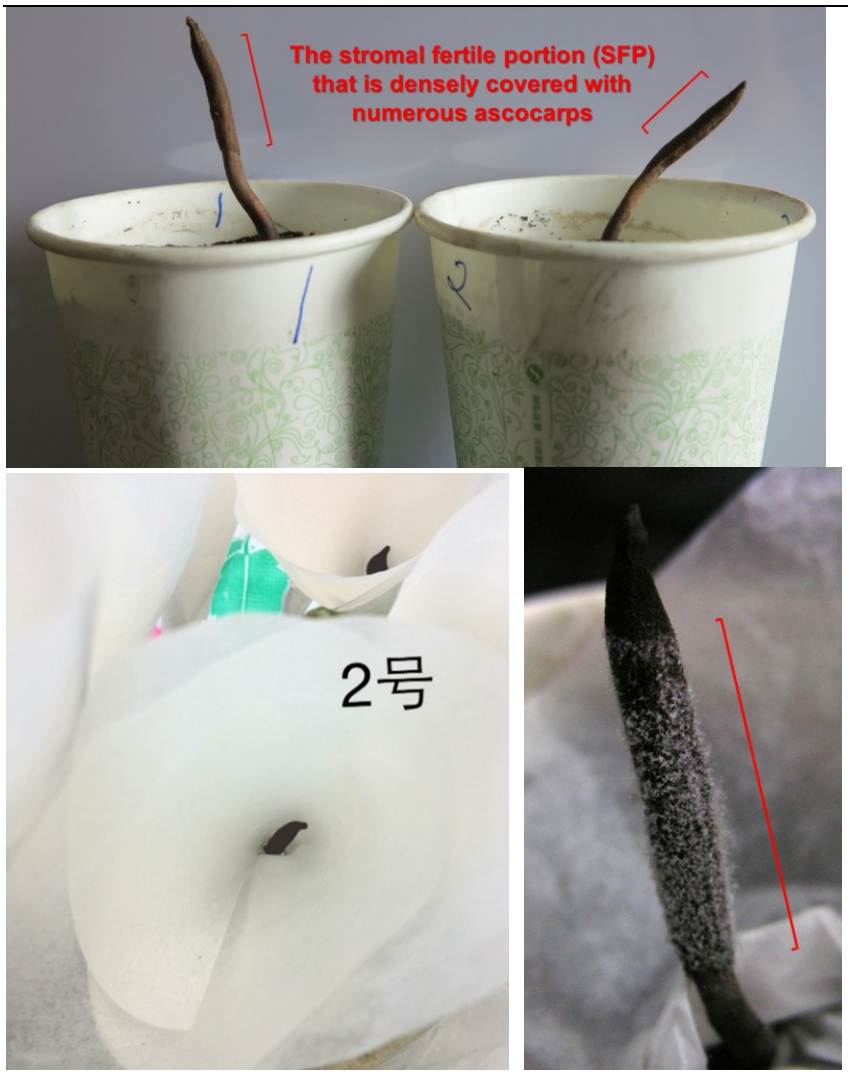

Fig 1. Cultivation of mature *C. sinensis* specimens in paper cups and collection of ascospores. Mature *C. sinensis* specimens were cultivated in our Xining laboratory (altitude of 2,200 m) (upper panel). The fully ejected ascospores were collected using the double layers of autoclaved weighing papers (lower-left panel). Numerous semiejected ascospores adhere to the outer surface of an ascus (lower-right panel, after removing the upper layer of autoclaved weighing papers for collection of the fully ejected ascospores) during the massive ejection of ascospores. The stromal fertile portion (SFP) densely covered with numerous ascocarps is labeled with "]".

Some of the mature *C. sinensis* specimens were harvested along with the outer mycelial cortices and soil surrounding the caterpillar body and replanted in paper cups in soil obtained from *C. sinensis* production areas (upper panel of Fig 1) and were cultivated in our laboratory (altitude 2,200 m) in Xining City, Qinghai Province of China [68–69]. Because of the phototropism of natural *C. sinensis*, we kept the windows fully open, allowing sufficient sunshine and a natural plateau breeze blowing over the cultivated specimens in the paper cups. The room temperature was maintained naturally, fluctuating with the lowest temperature at 18−19°C during the night and the highest temperature at 22−23°C in the early afternoon.

171 The humidity of our laboratory was maintained by spraying of water using an atomizer twice a day in the
172 morning and evening.

173 Fully ejected ascospores of *C. sinensis* were collected using double layers of autoclaved weighing
174 paper (lower-left panel of Fig 1). During massive ascospore ejection, numerous ascospores adhered to the
175 outer surface of asci, as shown in the lower-right panel of Fig 1 after removing the upper layer of
176 autoclaved weighing papers for collection of the fully ejected ascospores, and failed to be brushed away
177 using an autoclaved brush; hence, these ascospores were instead gently scratched off using a disinfected
178 inoculation shovel or ring and referred to as semiejected ascospores.

179 The 2 types of ascospores were cleaned by 2 washes with 10% and 20% sucrose solutions and 10-
180 min centrifugation at 1,000 rpm (desktop centrifuge, Eppendorf, Germany); the supernatant was discarded
181 after each centrifugation. The pellets (ascospores) were subsequently washed with 50% sucrose solution
182 and centrifuged for 30 min, and the ascospores that floated on the liquid were collected [68]. The fully
183 and semiejected ascospores were stored in a -80°C freezer prior to further processing.

184

185 Histological examination of the SFP, ascocarps and ascospores of *C.* 186 *sinensis*

187 The fully ejected ascospores of *C. sinensis* were diluted in normal saline, placed on a glass slide,
188 and air-dried for histological examination under an optical microscope (Model BX51, OLYMPUS, Japan)
189 without staining. The ascospores were fixed on a glass slide with 4% paraformaldehyde for 1 h, incubated
190 in 0.01% calmodulin for 5 min for the visualization of septa, washed 3 times with PBS, and observed
191 under a fluorescence microscope with UV epi-illumination (Model XZ51, OLYMPUS, Japan) [69].

192 The mature *C. sinensis* stromata collected during the massive ejection of ascospores were immersed
193 in 10% formalin for fixation and subjected to dehydration in 50%, 70% and 95% ethanol for 1 h each [70].
194 The SFP tissues (densely covered with ascocarps) were embedded in paraffin and sliced to 5-μm thickness
195 (Model TN7000 Microtome, Tanner Scientific, Germany). The ascus slices were stained with
196 hematoxylin-eosin and observed under optical and confocal microscopes (Model Primo Star and Model
197 LSM780, ZEISS, Germany).

198

199 ## Extraction and preparation of genomic DNA

200 The frozen test samples, including the stroma, SFP (densely covered with ascocarps), and the 2 types
201 of ascospores of *C. sinensis*, were individually ground to a powder in liquid nitrogen. The mycelia of pure
202 fungi, including *H. sinensis* and *Samsoniella hepiali* (synonym *Paecilomyces hepiali* [71]) (gifts from Prof.
203 Guo Y-L [26]), *Geomyces pannorum*, *Penicillium chrysogenum* and *Pseudogymnoascus roseus* (gifts
204 from Prof. Zhang Y-J), and *Tolypocladium sinensis* (provided by Prof. Wu J-Y), were also individually
205 ground to powder in liquid nitrogen; these fungi have been frequently detected in natural *C. sinensis*, and
206 some of them reportedly show differential dominance in the stroma and caterpillar body of *C. sinensis*
207 [23,26–29,36,38–41,72–74]. Genomic DNA was individually extracted from these powder samples using
208 the DNeasy Plant Mini Kit (Qiagen) according to the manufacturer's manual [19,26].

209

210 ## Universal primers and genotype- and species-specific primers

211 Table 1 lists the sequences of the *IST5/ITS4* universal primers, fungal species-specific primers and
212 the genotype-specific primers for GC- and AT-biased genotypes of *O. sinensis*. The positions of the
213 genotype-specific primers are shown in Fig 2. All primers were synthesized by Invitrogen Beijing Lab. or
214 Beijing Bomaide Technology Co.

215

216 **Table 1. ITS5/ITS4 universal primers and genotype- and species-specific primers used for the**
217 **PCR amplification and sequencing of ITS segments.**

Primer	Direction	Primer sequence
Universal Primers		
ITS5	Forward	GGAAGTAAAAGTCGTAACAAGG
ITS4	Reverse	TCCTCCGCTTATTGATATGC
Genotype-specific primers designed based on AB067721 of the GC-biased Genotype #1 *H. sinensis*		
Hsprp1	Forward	ATTATCGAGTCACCACTCCCAAACCCCC
Hsprp2	Reverse	ATTTGCTTGCTTCTTGACTGAGAGATGCC
Hsprp3	Reverse	CGAGGTTCTCAGCGAGCTACT
Genotype-specific primers designed based on AB067744 and AB067740 of the AT-biased *O. sinensis* genotypes		
HsATp1	Forward	AAGGTCTCCGTTAGTAAACT
HsATp2	Reverse	GGGGCTCGAGGGTTAAGATA
HsATp3	Reverse	GGGGCTTAAGGGTTAAGGTA
Species-specific primers designed based on DQ189229 of *Geomyces pannorum* and AY608922 of *Pseudogymnoascus roseus*		
Prp2	Forward	ATTACACTTTGTTGCTTTGGCA
Prp5	Reverse	GCTGGCGAGCACACGACCGGACCT
Species-specific primers designed based on DQ336710 of *Penicillium chrysogenum*		
Pcp3	Forward	GAGGGCCCTCTGGGTCCAACC
Pcp7	Reverse	CCCCATACGCTCGAGGACC
Species-specific primers designed based on EF555097 of *Samoneilla hepiali* (≡*Paecilomyces hepiali*)		
Php4	Forward	GTATCTTCTGAATCCGCCGCAAGGC
Php6	Reverse	AACGTTCAGAAGTCGGGGGTTTTAC
Species-specific primers designed based on DQ097715 of *Tolypocladium sinensis*		
Tsp1	Forward	GACCGCCCCGGCGCCCTCG
Tsp3	Reverse	TGACCGTCTCCGCGCT
Primers used for PCR2.1 vector clone sequencing		
M13F	Forward	TGTAAAACGACGGCGT
M13R	Reverse	CAGGAAACAGCTATCC

218

```
                          1         ITS5              HsATp1                            Hsprp1                          100
GT1   AB067721    1       TAGAGGAAGTAAAAGTCGTAACAAGGTCTCCGTTGGTGAACCAGCGGAGGGATCATTATCGAGTCACCACTCCCAAACCCCCTGCGAACACCACAGCAGT
JAAVMX010000017 9695      ------------------------------------------------------------------------------------------------------
LKHE01000582    2074      ------------------------------------------------------------------------------------------------------
ANOV01021709    838       -------------------------C----------------------------------------------------------------------------
LWBQ01000008  991739      ------------------------------------------------------------------------------------------------------
GT2   MG770309
GT3   HM595984    1                                 ---------------------------------CT----TG-----------A----C-T---------------
GT4   AB067744    1             ------------------AAGGTCTCCGTTAGTAAACT-----------T----------T-------T--------------T--T-------
GT5   AB067740    1       --A------------------T------------A--A---T-----------T----------T--T----TT---------ATA--T--T-T------
GT6   EU555436    1                                                                                                --T--T-T------
GT15  KT232017    1                                  ------------A--A---T-----------T----------T-------T--------------T--T-T------
GT16  KT232019    1                                  ------------A--A---T-----------T----------T--T----T--------------T--T-T------
GT17  KT232010    1                                  ------------A--A---T-----------T----------T--T----T--------------T--T-T------

                          101                                                                   Hsprp2 (RC)                 200
GT1   AB067721    101     TGCCTCGGCGGGACCGCCCCGGCGCCCCAGGGCCCGGACCAGGGCGCCCGCCGGAGGACCCCCAGACCCTCCTGTCGCAGTGGCATCTCTCAGTCAAGAA
JAAVMX010000017 9595      ------------------------------------------------------------------------------------------------------
LKHE01000582    2174      ------------------------------------------------------------------------------------------------------
ANOV01021709    938       ------------------------------------------------------------------------------------------------------
LWBQ01000008  991839      ------------------------------------------------------------------------------------------------------
GT2   MG770309    284                                                                   ----C------C-A-----------T-------------
GT3   HM595984    75      ---------------------------------------T-------------------------------------------G---------------
GT4   AB067744    97      ---------------------------T-----------T--------------------TT----------A---T---A--------T---T-----
GT5   AB067740    101     -----TA------------TA------T-A---------T-AA------------------TT----------A-TAT---A-T------T---T-----
GT6   EU555436    15      -----TA------------TA------T-A---------T--------------------TT----------A---T---A-T------T---T-----
GT15  KT232017    78      ---------------------------T-----------T--------------------TT----------A-------A--------T---T-----
GT16  KT232019    78      -----TA------------TA------T-A-A-------T-AA------------------TT----------A-------A-T------T---T-----
GT17  KT232010    78      -----TA------------TA------T-A---------T-AA------------------TT----------A-TAT---A-T------T---T-----

                          201                                                                                               300
GT1   AB067721    201     GCAAGCAAATGAATCAAAACTTTCAACAACGGATCTCTTGGTTCTGGCATCGATGAAGAACGCAGCGAAATGCGATAAGTAATGTGAATTGCAGAATTCA
JAAVMX010000017 9495      ------------------------------------------------------------------------------------------------------
LKHE01000582    2274      ------------------------------------------------------------------------------------------------------
ANOV01021709    1038      ------------------------------------------------------------------------------------------------------
LWBQ01000008  991939      ------------------------------------------------------------------------------------------------------
GT2   MG770309    245     ------------------------------------------------------------GA--------- C---------------------------
GT3   HM595984    175     ------------------------------------------------------------------------------------------------------
GT4   AB067744    197     ----------A---T--------T--T------------A---T-A----TA--A----------------A-------------A-----T------T-
GT5   AB067740    201     ----------A---T--------T--------------A-----A----TA--A--A---------------A---------A-A----A-------T-
GT6   EU555436    115     ----------A---T--------T--------------A-----A--------A-------T--TA----------------A-A----A-------T-
GT15  KT232017    178     --------------T--------T--T------------A---T-A----TA--A----------------A-------------A-----T------T-
GT16  KT232019    178     ----------A---T--------T--------------A-----A--------A--A---------------A---------A-A----A-------T-
GT17  KT232010    178     ----------A---T--------T--------------A-----A--------A--A---------------A---------A-A----A-------T-

                          301                                                                 HsATp2/HsATp3 (RC)            400
GT1   AB067721    301     GTGAACCATCGAATCTTTGAACGCACATTGCGCCCGCCAGCACTCTGGCGGGCATGCCTGTCCGAGCGTCATCTCAACCCTCGAGCCCCCCGCCTCGCGG
JAAVMX010000017 9395      ------------------------------------------------------------------------------------------------------
LKHE01000582    2374      ------------------------------------------------------------------------------------------------------
ANOV01021709    1138      ------------------------------------------------------------------------------------------------------
LWBQ01000008  992039      ------------------------------------------------------------------------------------------------------
GT2   MG770309    146     ------------------------------------------------------------------------------------------------------
GT3   HM595984    275     ---------------------------------------------A--------------------------------------------------------
GT4   AB067744    297     --A---T-----------A----T-T-C-A-------T--------A----------------------TACCTTAACCCTTAAGCCCC-----------
GT5   AB067740    301     --A---T-----------A------T---A-------T--------A------------A---------TATCTTAACCCTCGAGCCCC-----------
GT6   EU555436    215     --A---------------A----T-T---A-------T--------A----------------------T----T--------------------TA---
GT15  KT232017    278     --A---T-----------A----T-T---A-------T--------A----------------------T----T-------------------------
GT16  KT232019    278     --A---T-----------A----T-T---A-------T--------A----------------------T-C--T------TA-----------------
GT17  KT232010    278     --A---T-----------A------T-----------T--------A------------A---------T----T-------------------------

                          401                                                                                 Hsprp3 (RC)  500
GT1   AB067721    401     CGGCGGGGCCCGGCCTTGGGGGTCACGGCCCCGCGCCGCCCCCTAAACGCAGTGGCGACCCCGCCGCGGCTCCCCTGCGCAGTAGCTCGCTGAG AACCT
JAAVMX010000017 9295      ------------------------------------------------------------------------------------------------ -----
LKHE01000582    2474      ------------------------------------------------------------------------------------------------ -----
ANOV01021709    1238      ---G--------------------------------------------------------------------------------------------- -----
LWBQ01000008  992139      ------------------------------------------------------------------------------------------------ -----
GT2   MG770309    46      ---------------------------------------------
GT3   HM595984    375     --A---------------------------T---------------T---------------------------------------C---G-----
GT4   AB067744    397     ----------------A-------------A-------------------A-T-------------------A---A-----TA--A-- -----
GT5   AB067740    401     ---------T-------A-----T-----------------T------T---A---------------------A--TG------A-C--- -----
GT6   EU555436    315     ---------T-------A-----T-----------------T---------A-------T----TA-------ATAT-------TA-C--- -----
GT15  KT232017    378     ---------T-------A-----T---------------------------T---A---------------------A--T-A------A-C--- -----
GT16  KT232019    378     -----------------A--------------A-------------------A------------------T---A----A-----TA--A-- -----
GT17  KT232010    378     ---------T-------A-----T---------------------------T---A---------------------A--T-A------A-C--- -----

                          501                                                                                       ITS4(RC)600
GT1   AB067721    500     CGCACCGGGAGCGCGGAGGCGGTCACGCCGTGAAACCACCACACCCTCCAGTTGACCTCGGATCAGGTAGGGATACCCGCTGAACTTAAGCATATCAATA
JAAVMX010000017 9194      ------------------------------------------------------------------------------------------------------
LKHE01000582    2573      ------------------------------------------------------------------------------------------------------
ANOV01021709    1337      ------------------------------------------------------------------------------------------------------
LWBQ01000008  992238      ---CT--C------------------------------------------------------------------------------------------------
GT2   MG770309    1
GT3   HM595984    475     --------A-------G--T----------C------------    ----------
GT4   AB067744    496     -----TA-----------------------A-------T-T------TG---A---------T-----------------A------------------
GT5   AB067740    500     --------A----------------------A-----T-T--G--T-TT----A---------T-----------------A-------------T----
GT6   EU555436    414     --------A---A-------TA-A-------T-CG--T--TAG--
GT15  KT232017    477     --------A----------------------A-------T--G--T-TT----A---------T-----------------A------------------
GT16  KT232019    477     -----TA-----------------------A-------T-T------T----A---C-----T-A---------------A------------------
GT17  KT232010    477     --------A----------------------A-------T--G--T-TT----A---------T-----------------A------------------

                          601                                                                                 686
GT1   AB067721    600     AGCGGAGGAAAAGAAACCAACAGGGATTGCCCCAGTAACGGCGAGTGAAGCGGCAACAGCTCAAATTT
JAAVMX010000017 9094      ------------------------------------------------------------------
LKHE01000582    2673      ------------------------------------------------------------------
ANOV01021709    1437      ------------------------------------------------------------------
LWBQ01000008  992338      ------------------------------------------------------------------
GT2   MG770309    1
GT3   HM595984    518
GT4   AB067744    596     ---------
GT5   AB067740    600     -----------------T--T----------TT-------------A------T--T----T------AAAATCTAGCCCCCCTACG
GT6   EU555436    467
GT15  KT232017    577     ---------
GT16  KT232019    577     ---------
GT17  KT232010    577     ---------
```

Fig 2. Alignment of the ITS sequences of GC- and AT-biased genotypes of *O. sinensis* with multiple transition point mutations. GT represents genotype. Genotypes #1–3 are GC-biased *O. sinensis* genotypes, and Genotypes #4–6 and #15–17 are AT-biased *O. sinensis* genotypes. The sequence segments shown in blue correspond to the primers designed based on the sequences of GC-biased genotypes, and those in red correspond to primers designed based on the sequences of AT-biased genotypes. The underlined "GAATTC" site shown in green is the enzymatic site of the *Eco*RI endonuclease, and it is present in the GC-biased sequences at nucleotides 294–299 in Genotype #1 but absent in the AT-biased sequences due to a single-base mutation (GAATTT). "(RC)" denotes the reverse complement sequence of the primers; "-" represents identical bases; and spaces indicate unmatched sequence gaps.

Among multiple pairs of species-specific primers that were designed for *G. pannorum*, *H. sinensis*, *P. chrysogenum*, *P. roseus*, *S. hepiali* and *T. sinensis*, the following primer pairs were selected according to their specificity and amplification efficiency as examined through PCR amplification and sequencing using the genomic DNA templates isolated from the fungal mycelia (listed in Table 1): *Prp2/Prp5* for *G. pannorum* and *P. roseus*, *Pcp3/Pcp7* for *P. chrysogenum*, *Php4/Php6* for *S. hepiali*, and *Tsp1/Tsp3* for *T. sinensis*. The ITS sequences of *P. roseus* (AY608922) and *G. pannorum* (JF320819 and DQ189229) are 98–99% homologous and were amplified using the same pair of primers, *Prp2/Prp5* (Table 1).

PCR protocol for the amplification of ITS segments

The genomic DNA templates and aforementioned universal, genotype- and species-specific primers were used in PCR assays using a PCR instrument (Bio-Rad, United States) and *Taq* PCR reagent kit (Invitrogen) to amplify the ITS1-5.8S-ITS2 segments using the following touch-down protocol: (1) 95°C for 5 min; (2) 36 cycles of 95°C for 30 sec, annealing temperature for 30 sec (the annealing temperature was initially set to 70°C and decreased stepwise by 0.3°C in each cycle), and 72°C for 1 min; (3) 72°C for 10 min and final incubation at 4°C [26–27]. The PCR amplicons were examined by agarose gel electrophoresis and sequencing.

Amplicon sequencing, cloning-based sequencing and sequence analysis

Each of the targeted PCR amplicons obtained from the aforementioned genomic DNA templates was recovered from agarose gels using a Gel Extraction Kit (Omega Bio-Tek) and purified using a Universal DNA Purification kit (TIANGEN) according to the manufacturer's manuals [26–27]. The

250 purified amplicons were subjected to *Eco*RI endonuclease (BioLabs) digestion, which specifically
251 digested the GC-biased genotypes of *O. sinensis* but not the AT-biased genotypes (*cf*. the underlined
252 "GAATTC" site in green shown in Fig 2) and analyzed by agarose gel electrophoresis. The purified
253 amplicons were sequenced either directly or after cloning by Invitrogen Beijing Lab.

254 For cloning, the amplicon was inserted into a PCR2.1 vector (SHQIMBIO, Shanghai, China), which
255 was then transfected into DH5α cells, and the cells were coated on agar containing 100 μg/mL ampicillin
256 or kanamycin in Petri dishes. The Petri dishes were cultured at 37°C, allowing the growth of cells; 30
257 white colonies were selected per dish, transferred to liquid culture medium and grown at 37°C in a shaking
258 incubator. The expanded clones were sequenced using the M13F/M13R primers (*cf*. Table 1) (Invitrogen
259 or Beijing Bomaide Technology Co.). The sequences were analyzed using Vector NTI Advance 9 software
260 (Invitrogen) [26–27].

261

262 Phylogenetic analysis of ITS sequences

263 All 17 genotypes of *O. sinensis* available in the GenBank database and obtained from this study
264 were analyzed by Nanjing Genepioneer Biotechnologies Co. to reveal their phylogenetic relationships. A
265 Bayesian majority-rule consensus tree was inferred using MrBayes v3.2.7a software (the Markov chain
266 Monte Carlo [MCMC] algorithm; http://nbisweden.github.io/MrBayes/) with a sampling frequency of 10^3
267 iterations after discarding the first 25% of samples from a total of 1.1×10^8 iterations [75].

268

269

270 Results

271 Two types of *C. sinensis* ascospores

272 To mimic the wild environment of the Qinghai-Tibetan Plateau, mature *C. sinensis* specimens were
273 cultivated in paper cups in our Xining laboratory (altitude 2,200 m) (upper panel of Fig 1). White
274 ascospores started to become visible on the surface of asci after approximately one week of cultivation.
275 The fully ejected ascospores were collected on the double layers of autoclaved weighing paper (lower-left
276 panel of Fig 1), and the numerous semiejected ascospores that tightly adhered to the outer surface of asci
277 (lower-right panel of Fig 1 after removing the upper layer of autoclaved weighing papers for collection of

the fully ejected ascospores) were collected by gentle scraping using a disinfected inoculation shovel or ring [68].

Microscopy observations of the SFPs, ascocarps and ascospores of *C. sinensis*

Fig 3 shows the histology of the fully ejected *C. sinensis* ascospores without staining (upper panel; 40x) and after staining with calmodulin to visualize the septa of the multicellular structure of the ascospores (lower panel; 400x).

Fig 3. Microscopy images of fully ejected ascospores of *C. sinensis* without staining (upper panel; 40x) or after staining with 0.01% calmodulin for visualization of the septa of multicellular ascospores (lower panel; 400x).

Panel 4A of Fig 4 shows a confocal image (bar, 500 μm) of a transverse section of the fertile portion of the *C. sinensis* stroma, which is densely covered with multiple ascocarps. Panel 4B shows an optical microscopy image (10x) of several ascocarps, and Panel 4C shows a close-up optical microscopy image (40x) of an ascocarp. Ascocarps were stained with hematoxylin-eosin containing multiple ascospores, which revealed uneven staining of nuclei (dark blue–purple), consistent with the multicellular heterokaryosis of the *C. sinensis* ascospores reported by Bushley et al. [76]. Panels 4D and 4E provide confocal images close to the opening of the perithecia, showing ascospores gathering toward the opening

297 of the perithecium (4D; bar, 50 µm) and a semiejected ascospore hanging out and adhered to the opening
298 of the perithecium (4E; bar, 20 µm). Arrows in Panels 4B and 4E indicate semiejected ascospores.

299 4A

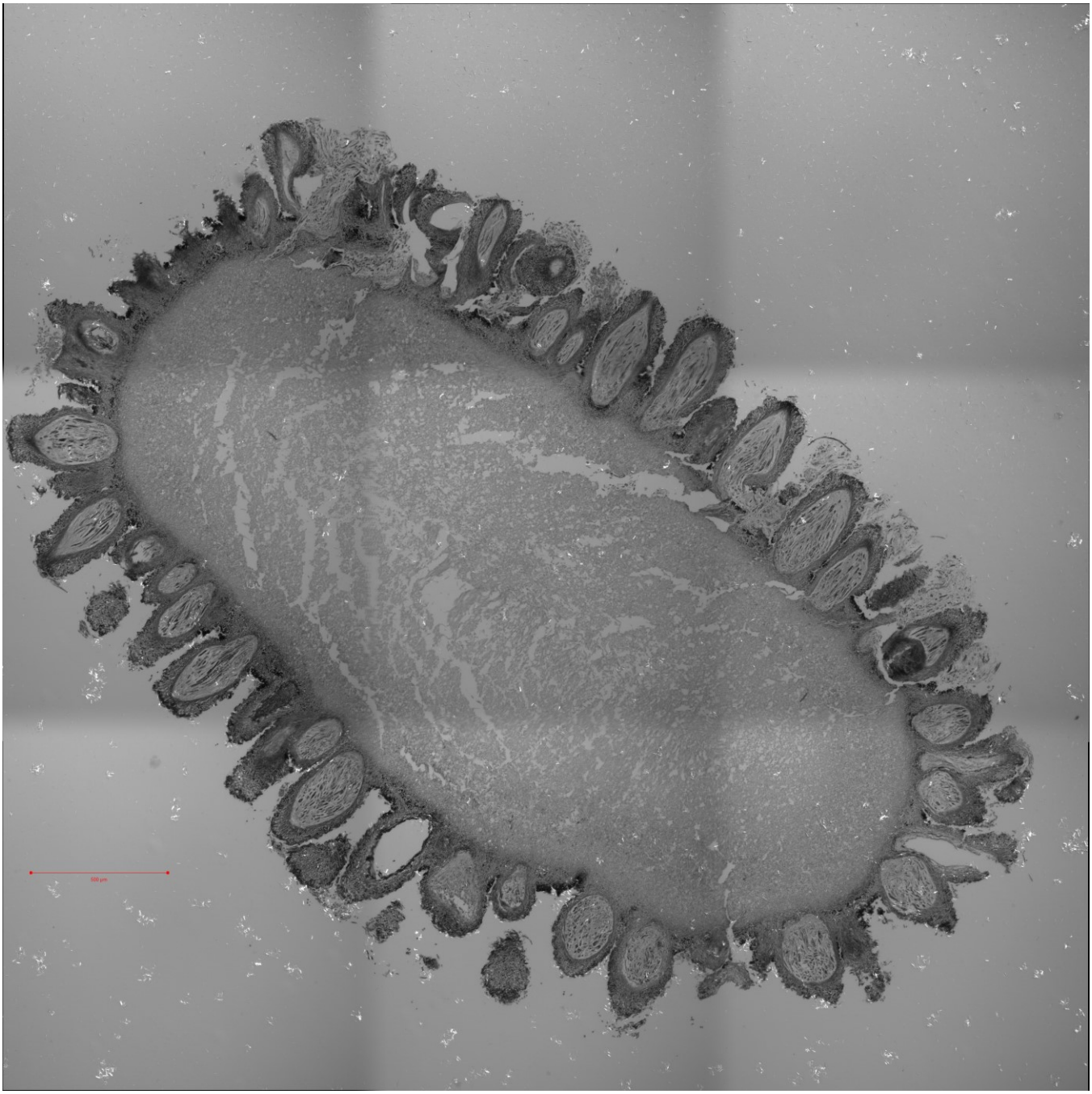

300
301

4B

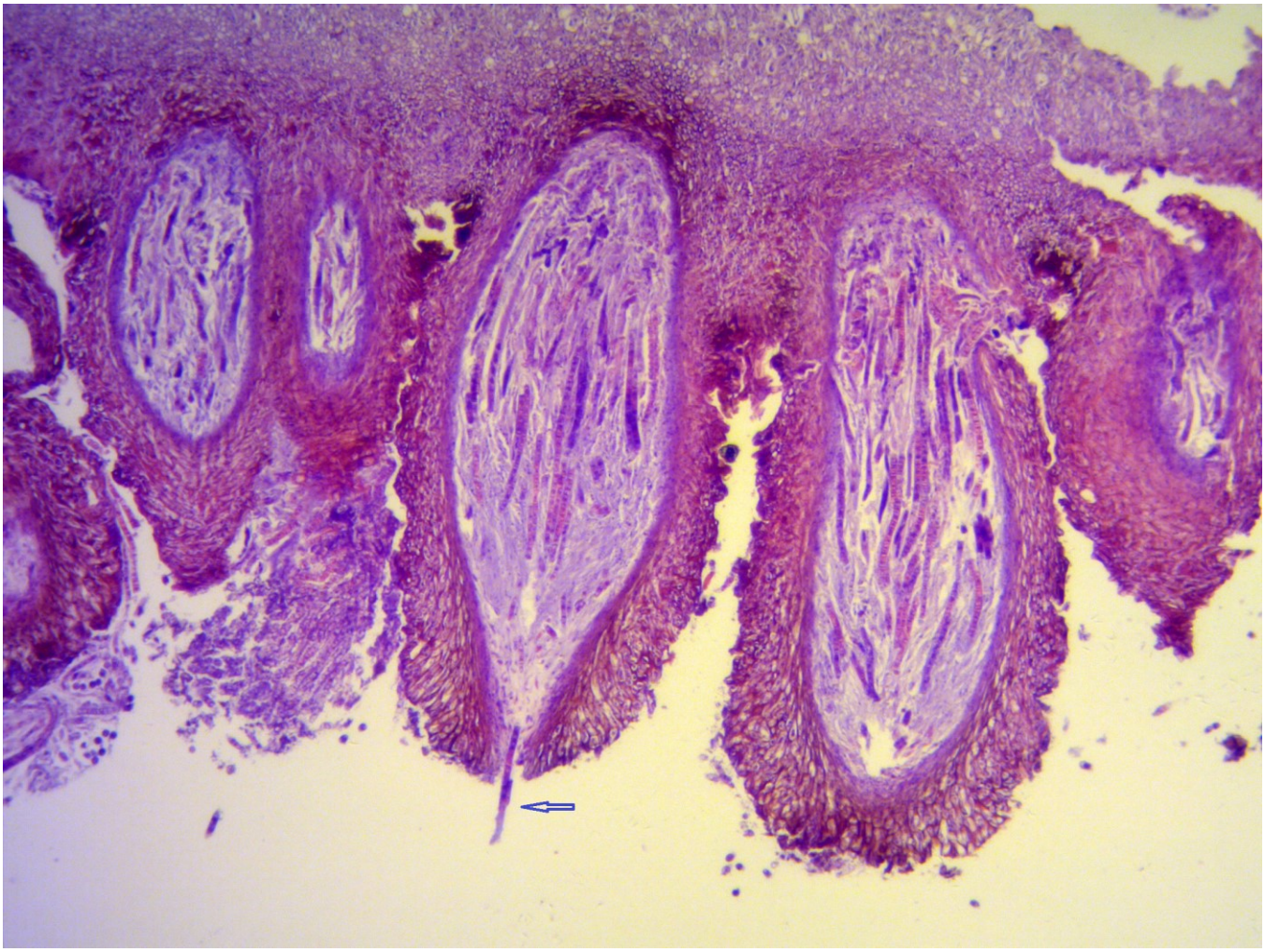

4C

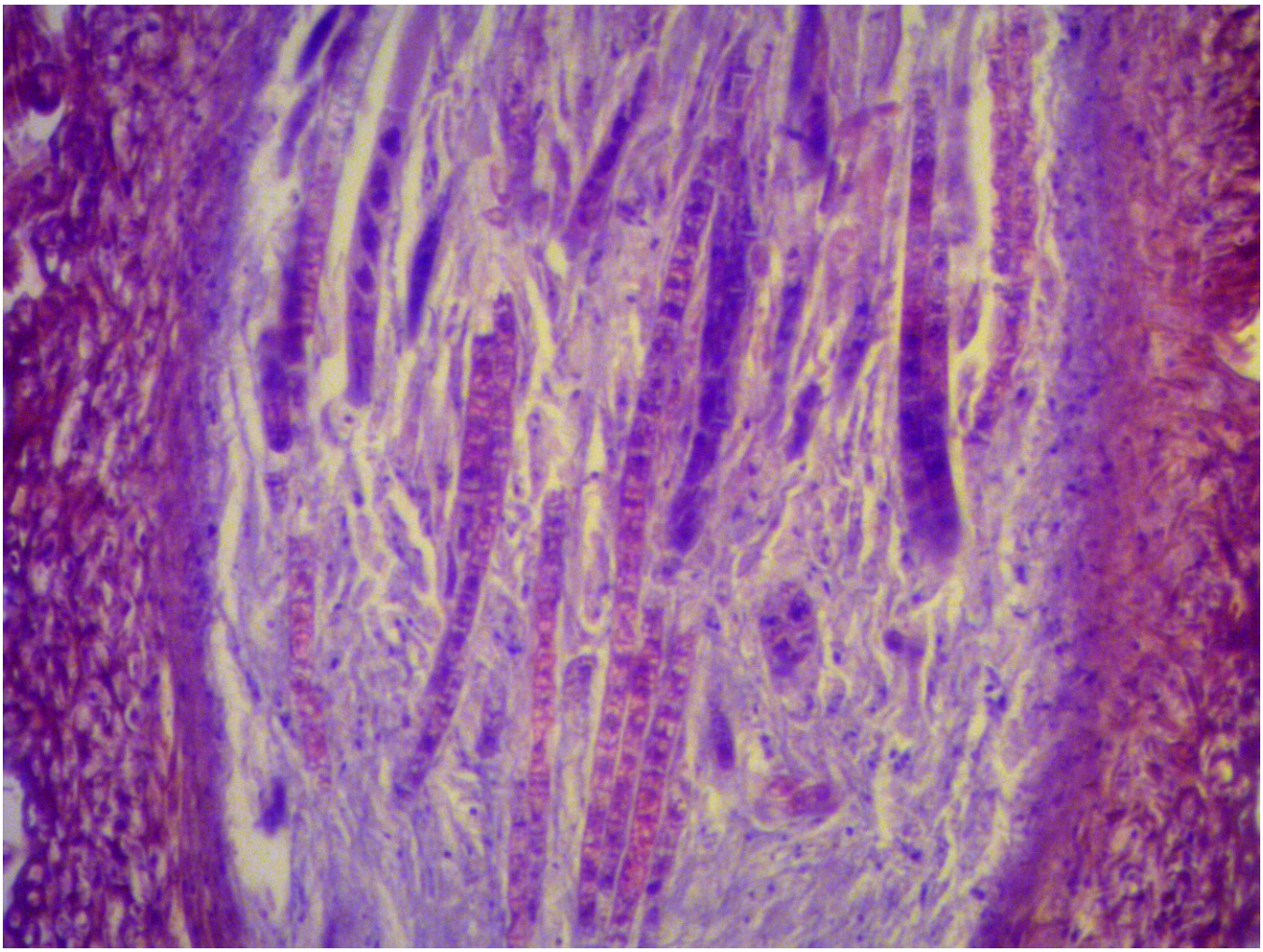

4D

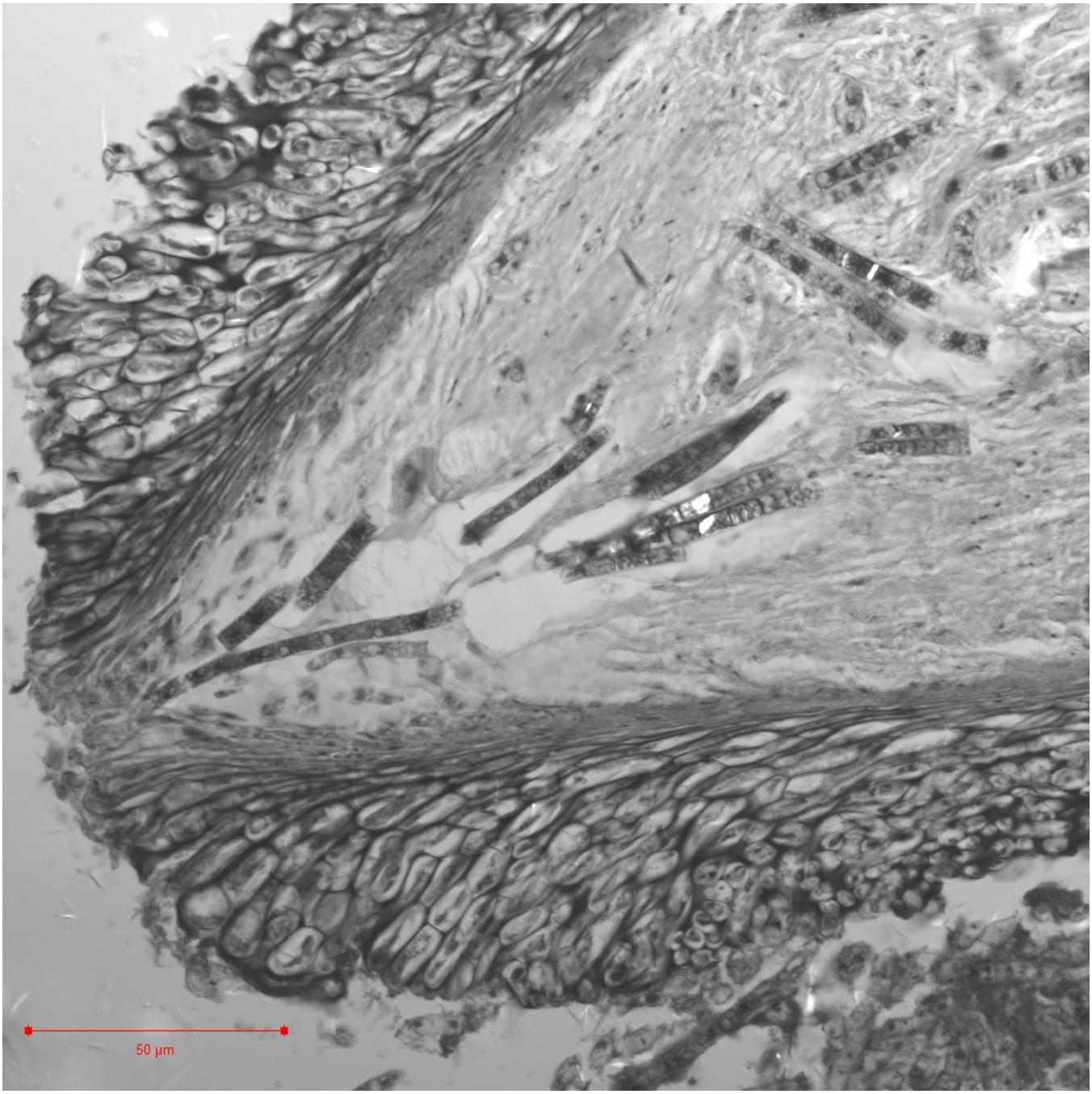

4E

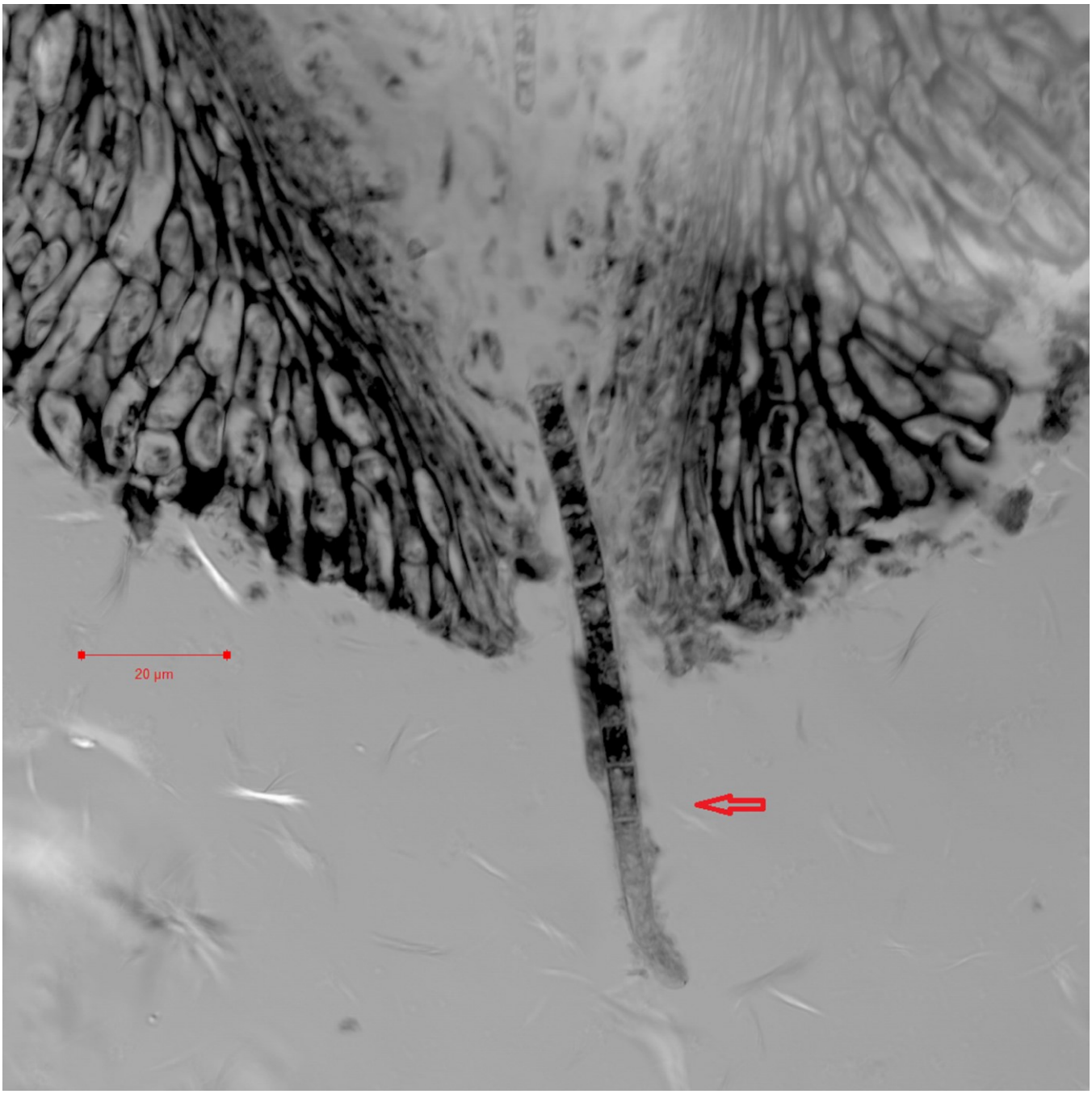

Fig 4. Microscopy images of the SFP, ascocarps and ascospores of *C. sinensis*. Panel 4A is a confocal image of a transverse section of the SFP (bar, 500 µm). Panel 4B is an optical microscopic image (10x) of several *C. sinensis* ascocarps stained with hematoxylin-eosin. Panel 4C is a close-up optical image (40x) of an ascocarp stained with hematoxylin-eosin. Panels 4D and 4E are close-up confocal images showing ascospores gathering toward the opening of the perithecium (4D; bar, 50 µm) and a semiejected ascospore hanging out of the opening of the perithecium (4E; bar, 20 µm). Arrows in Panels 4B and 4E indicate semiejected ascospores.

ITS sequences amplified using universal primers

ITS sequences were amplified from the immature and mature stroma, SFP (with ascocarps), and fully and semiejected ascospores of *C. sinensis* using the universal primers *ITS5/ITS4*. The targeted amplicons of 630^{+} bp are 99% homologous to sequence AB067721 of *H. sinensis* (Genotype #1 of *O. sinensis*) [18,23–24,26–27,33,35,37,44,48].

ITS sequences amplified using species-specific primers

ITS sequences were amplified from the genomic DNA templates obtained from immature and mature stroma, SFP (with ascocarps), and fully and semiejected ascospores of *C. sinensis* using the *S. hepiali*-specific primers *Php4/Php6*. The targeted amplicons of 460^{+} bp in the sample lanes shown in Fig 5 were recovered and sequenced, and the sequences were 100% homologous to the EF555097 sequence of *S. hepiali* [26]. As determined through PCR amplification of the same quantity of genomic DNA, significantly lower abundance of the moieties of the ITS amplicons was obtained after amplification from genomic DNA of the fully ejected ascospores (lanes 1 and 3 of Fig 5) than after amplification of genomic DNA of the semiejected ascospores (lanes 2 and 4).

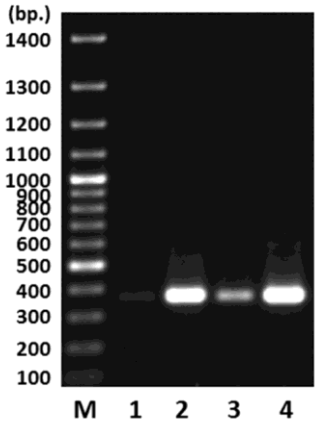

Fig 5. Agarose gel electrophoresis of the PCR amplicons obtained from genomic DNA of the fully and semiejected ascospores of *C. sinensis* using the *Samsoniella hepiali*-specific Php4/Php6 primers. Lane M shows the molecular weight standard. Lanes 1 and 3 display the amplicon moieties amplified from the genomic DNA of the fully ejected ascospores. Lanes 2 and 4 show the amplicons amplified from the genomic DNA of the semiejected ascospores.

In other PCR experiments, the ITS sequences of various fungi were amplified from the SFP (with ascocarps) and fully and semiejected ascospores of *C. sinensis* using the following species-specific primer

346 pairs (*cf*. Table 1): *Prp2/Prp5* for *G. pannorum* (JF320819) and *P. roseus* (AY608922), *Pcp3/Pcp7* for *P.*
347 *chrysogenum* (DQ336710), and *Tsp1/Tsp3* for *T. sinensis* (DQ097715) (*cf*. Table 1). Amplicon sequencing
348 did not detect the sequences of *G. pannorum*, *P. roseus*, or *T. sinensis*. Agarose gel electrophoresis showed
349 that the amplicons obtained using the primers *Pcp3/Pcp7* migrated at a speed similar to the positive control
350 moiety of *P. chrysogenum*, but sequencing analysis did not reveal the ITS sequence of *P. chrysogenum*.
351 Thus, species-specific PCR primers failed to detect the ITS sequences of *G. pannorum*, *P. chrysogenum*,
352 *P. roseus*, or *T. sinensis* in the SFP (with ascocarps) and fully and semiejected ascospores of *C. sinensis*.
353

354 Profiling of multiple *O. sinensis* genotypes in the compartments of *C.* 355 *sinensis* using a cloning-based sequencing approach

356 Multiple genotypes of *O. sinensis* were further examined using genomic DNA obtained from the
357 immature and mature stromata, SFP (with ascocarps), and 2 types of ascospores of *C. sinensis*. Multiple
358 genotype-specific primers were designed and tested for specificity and amplification efficiency, and 5
359 pairs were selected for amplification of the ITS1-5.8S-ITS2 sequences of the GC- and AT-biased *O.*
360 *sinensis* genotypes (*cf*. Table 1). The universal primers *ITS5/ITS4* and the genotype-specific primer pairs
361 *Hsprp1/Hsprp2*, *Hsprp1/Hsprp3*, or *Hsprp2/Hsprp3* were highly homologous to GC-biased Genotypes
362 #1–2 and/or #7. The primer design did not consider GC-biased Genotypes #3 and #8–12 because the
363 sequences were obtained from *C. sinensis* specimens collected from Nyingchi of Tibet and the Indian-
364 Nepal side of the *C. sinensis* production areas, which are geographically distant from the sample collection
365 locations in Qinghai Province used for our study. The genotype-specific primer pairs *HsATp1/ITS4*,
366 *HsATp1/HsATp2*, and *HsATp1/HsATp3* were selected to amplify the AT-biased sequences of *O. sinensis*
367 (*cf*. Table 1 and Fig 2). The amplification specificity and efficiency of the primer pairings have been
368 previously tested repeatedly for the genotypes of *O. sinensis*. The PCR amplicons were subjected to
369 cloning-based sequencing to explore the multiple mutant genotypes.

370 The primer pair *HsATp1/ITS4* is highly homologous to almost all AT-biased genotype sequences
371 (100%/100%) but slightly less homologous to Genotype #5 (100%/95%) and AB067719-type sequences
372 (95%/100%). The primer pair *HsATp1/HsATp2* is highly homologous to sequences of Genotypes #5, #15
373 and #17 (100%/100%) but less specific for Genotypes #4 and #16 (100%/80%). The primer pair
374 *HsATp1/HsATp3* is highly homologous to Genotype #4 and #16 sequences (100%/100%) but less specific
375 for Genotypes #5, #15 and #17 sequences (100%/85%). The homology of the primer *HsATp1* to the

Genotype #6 sequence is unknown because all Genotype #6 sequences available in GenBank are short, probably due to the secondary structure/conformation within the ITS1 sequence close to its 5' end and the ITS2 sequence close to its 3' end. The primer *HsATp2* is 100% homologous to sequence EU555436 of Genotype #6, but *HsATp3* is less specific (85%) for EU555436. Thus, based on pretest and formal test results of the primer pairs in terms of the amplification specificity and efficiency, using all of these primer pairs in multiple PCR runs is essential for ensuring the successful amplification of all known genotypes of *O. sinensis* existing in the stroma, SFP (with ascocarps), and ascospores of *C. sinensis*.

Table 2 lists the differential occurrence of the *O. sinensis* genotypes with numerous transition point mutations detected in the immature and mature stromata, SFP (with ascocarps), and the 2 types of ascospores of *C. sinensis*. GC-biased Genotype #1 *H. sinensis* was identified in all compartments of *C. sinensis*. GC-biased Genotype #2 of *O. sinensis* was detected in both immature and mature stromata [27–28].

Table 2. Differential occurrence of multiple genotypes of *O. sinensis*, *S. hepiali* and AB067719-type fungus in the compartments of natural *C. sinensis*.

Genotype	Representative sequence	Stroma		SFP (with ascocarps)	Ascospores	
		Immature	Mature		Fully ejected	Semiejected
#1	AB067721	√	√	√	√	√
#2	MG770309	√	√			
#4	AB067744	√	√	√		
#5	AB067740	√	√	√	√	√
#6	EU555436	√	√	√	√	
#13	KT339190					√
#14	KT339178				√	
#15	KT232017	√	√	√		
#16	KT232019	√			√	
#17	KT232010	√				
S. hepiali	EF555097	√	√	√	√	√
AB067719-type fungus	AB067719	√	√	√	√	√

Zhang et al. [57] and Cheng et al. [58] studied *C. sinensis* specimens collected from the Nyingchi area in Tibet and detected variable *H. sinensis* sequences corresponding to Genotype #3 of *O. sinensis* [7–

12]. Chen et al. [60] detected a variable *H. sinensis* sequence AJ488254 (Genotype #7 of *O. sinensis*) in the stroma of a *C. sinensis* specimen (#H1023) collected from Qinghai Province of China, but Genotype #1 *H. sinensis* AJ488255 in the caterpillar body of the same specimen. In the current study, however, GC-biased Genotypes #3 and #7–12 were not detected in any compartments of natural *C. sinensis* collected from the Hualong and Yushu areas of Qinghai Province.

The cloning-based ITS amplicon sequencing approach showed the differential occurrence of the AT-biased sequences of Genotypes #4–6 and #15–17 of *O. sinensis* in the immature and mature stromata, SFP (with ascocarps), and 2 types of ascospores of *C. sinensis* (*cf*. Table 2). Table 2 also shows that *S. hepiali* and the AB067719-type fungus coexisted in the stromata, SFP (with ascocarps), and ascospores of *C. sinensis*.

Cloning-based amplicon sequencing also detected Genotypes #13–14 of *O. sinensis*. The Genotype #13 KT339190 sequence was detected in semiejected ascospores, whereas the Genotype #14 KT339178 sequence was detected in fully ejected ascospores (*cf*. Table 2). Table 3 compares the ITS1, 5.8S gene, and ITS2 segment sequences of the mutant genotypes with those of Genotype #1 *H. sinensis* (Group-A [66]) and the AB067719-type Group-E fungus. ITS1 of KT339190 and ITS2 of KT339178 are 100% homologous to those of Genotype #1 *H. sinensis* (AB067721). The 5.8S-ITS2 segments of KT339190 and ITS1-5.8S segments of KT339178 are 99–100% homologous to those of the AB067719-type fungus but 64.2–94.9% similar to those of the AB067721 of Genotype #1. As shown in Table 3 and Fig 6, the *O. sinensis* offspring Genotypes #13–14 resulted from large DNA segment reciprocal substitutions and genetic material recombination between the genomes of the 2 parental fungi, Group-A Genotype #1 *H. sinensis* and the AB067719-type Group-E fungus.

Table 3. Sequence similarities of the ITS1, 5.8S and ITS2 segments of Genotype #1 and AB067719-type sequences compared with the multiple genotypes of *O. sinensis*.

Genotype and representative sequence	ITS1	5.8S gene	ITS2	ITS1-5.8S-ITS2 (excluding the 18S and 28S segments)
	Genotype #1 (AB067721) *vs*. sequences of other genotypes			
#2 MG770309	83.6%	97.4%	100%	94.7%
#3 HM595984	94.3%	99.4%	93.0%	95.5%
#4 AB067744	90.6%	85.3%	89.2%	88.4%
#5 AB067740	80.5%	86.5%	89.2%	85.5%
#6 EU555436	84.7%	87.8%	85.8%	86.0%
#7 AJ488254	93.2%	98.7%	89.4%	93.9%
#8 GU246286	86.2%	94.8%	87.9%	89.6%
#9 GU246288	96.3%	98.7%	91.5%	95.3%
#10 GU246287	86.2%	92.9%	72.4%	83.2%
#11 JQ695935	94.3%	100%	55.1%	81.6%
#12 GU246296	99.4%	99.4%	87.0%	94.9%
#13 KT339190	**100%**	94.8%	64.2%	86.3%
#14 KT339178	67.9%	94.9%	**100%**	87.7%
#15 KT232017	91.8%	86.5%	91.7%	89.9%
#16 KT232019	84.3%	88.2%	90.7%	87.3%
#17 KT232010	83.0%	88.5%	91.7%	87.7%
	AB067719 (Group E) *vs*. sequences of Genotypes #13–14			
#13 KT339190	71.5%	**100%**	**99%**	88.2%
#14 KT339178	**100%**	**100%**	71.5%	89.2%

Fig 6. Schematic representation of the ITS segment sequences of the parental fungi (*H. sinensis* and the AB067719-type fungus) and *O. sinensis* offspring Genotypes #13–14. The green bars indicate the ITS1 segment; the pink bars refer to the 5.8S gene; the blue bars represent the ITS2 segment. AB067719 [34] and KT339197 discovered in the current study represent the AB067719-type Group-E fungus and are shown with

lighter bars. AB067721 [34] and KT339196 discovered in the current study represent Genotype #1 *H. sinensis* (Group-A by [66]) and are shown with darker bars. Alignment of the AB067719 and AB067721 sequences is shown between the lighter bars for AB067719 and the darker bars for AB067721. KT339190 and KT339178 represent *O. sinensis* offspring Genotypes #13 and #14, respectively, showing large DNA segment reciprocal substitutions and genetic material recombination between the genomes of the 2 parental fungi, *H. sinensis* and the AB067719-type fungus.

AB067719-type fungus in natural *C. sinensis* was grouped as a Group-E fungus by Stensrud et al. [66], unlike *O. sinensis* of Groups A–C. This fungus and 13 other sequences were annotated in the GenBank database as "*C. sinensis*" or "*O. sinensis*" under GenBank taxon 72228 for *C. sinensis* and *O. sinensis*. GenBank also collected more than 900 sequences highly homologous to AB067719, including *Alternaria* sp., *Ascomycota* sp., *Aspergillus* sp., *Avena* sp., *Berberis* sp., *Colletotrichum* sp., *Cordyceps* sp., *Cyanonectria* sp., *Dikarya* sp., *Fusarium* sp., *Gibberella* sp., *Hypocreales* sp., *Juglans* sp., *Lachnum* sp., *Nectria* sp., *Nectriaceae* sp., *Neonectria* sp., *Penicillium* sp., and many uncultured endophytic fungi. Thus, the identity of AB067719-type fungus in natural *C. sinensis* needs to be further determined through culture-dependent approaches and multigene and whole-genome sequencing of a purified AB067719-type fungus.

Phylogenetic relationship of the genotypes of *O. sinensis*

Kinjo & Zang [34] and Stensrud et al. [66] discussed the phylogenetic relationships of Genotype #1 (Group-A) and Genotypes #4–5 (Groups B–C) of *O. sinensis.* Further phylogenetic analysis of mutant genotypes #1–12 of *O. sinensis*, which share the same *H. sinensis*-like morphological and growth characteristics, reflected the research progress that had been achieved at the time [7–12,16–19,25,27–28,57–61]. In this study, we found additional AT-biased Genotypes #15–17 and GC-biased Genotypes #13–14 that show large DNA segment reciprocal substitutions and genetic material recombination (*cf.* Tables 2–3 and Fig 6). The sequences of all 17 *O. sinensis* genotypes were subjected to phylogenetic analysis using a Bayesian algorithm (Fig 7).

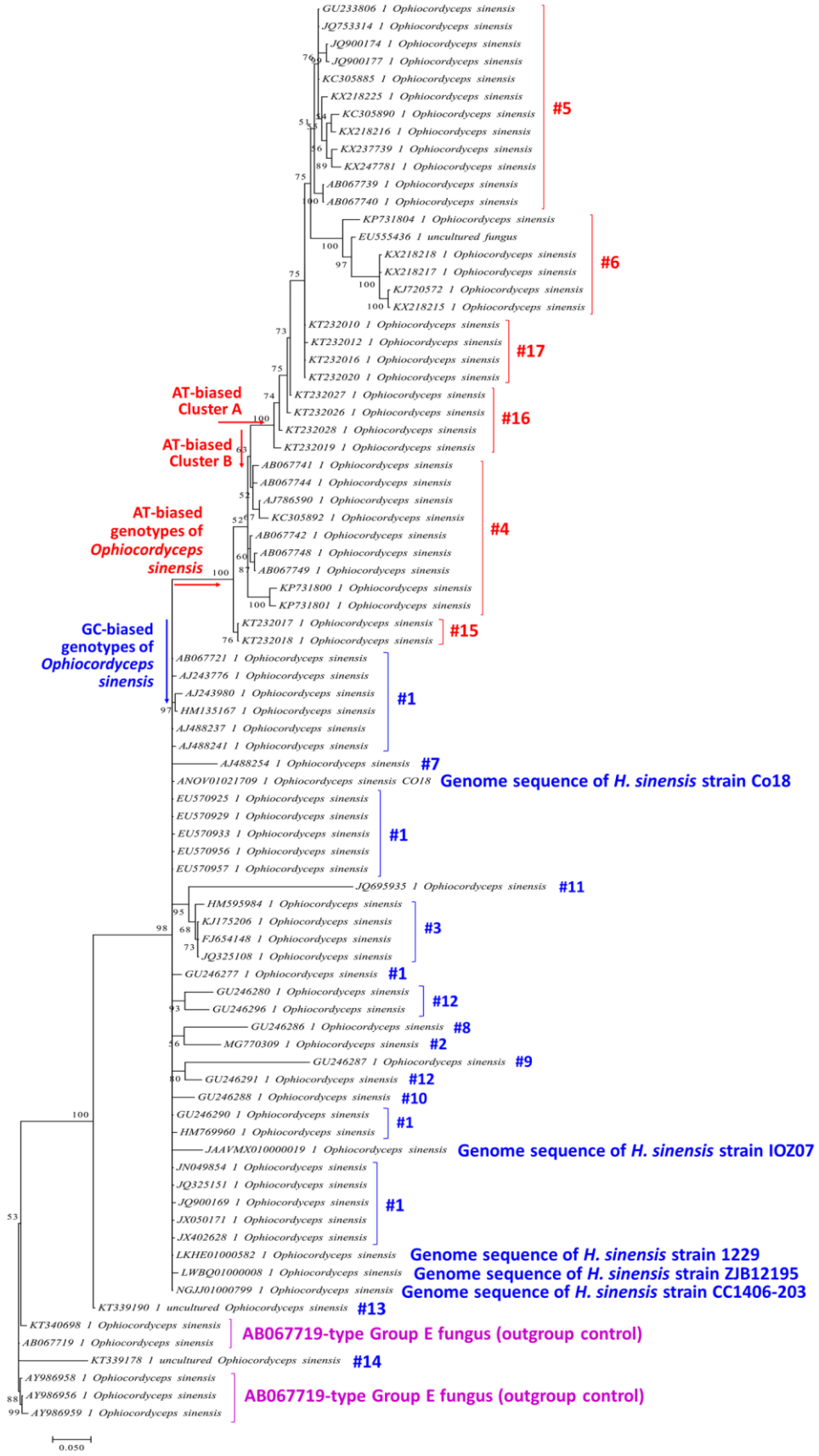
GU233806 1 Ophiocordyceps sinensis
JQ753314 1 Ophiocordyceps sinensis
JQ900174 1 Ophiocordyceps sinensis
JQ900177 1 Ophiocordyceps sinensis
KC305885 1 Ophiocordyceps sinensis
KX218225 1 Ophiocordyceps sinensis
KC305890 1 Ophiocordyceps sinensis
KX218216 1 Ophiocordyceps sinensis
KX237739 1 Ophiocordyceps sinensis
KX247781 1 Ophiocordyceps sinensis
AB067739 1 Ophiocordyceps sinensis
AB067740 1 Ophiocordyceps sinensis
#5
KP731804 1 Ophiocordyceps sinensis
EU555436 1 uncultured fungus
KX218218 1 Ophiocordyceps sinensis
KX218217 1 Ophiocordyceps sinensis
KJ720572 1 Ophiocordyceps sinensis
KX218215 1 Ophiocordyceps sinensis
#6
KT232010 1 Ophiocordyceps sinensis
KT232012 1 Ophiocordyceps sinensis
KT232016 1 Ophiocordyceps sinensis
KT232020 1 Ophiocordyceps sinensis
#17
AT-biased Cluster A
KT232027 1 Ophiocordyceps sinensis
KT232026 1 Ophiocordyceps sinensis
KT232028 1 Ophiocordyceps sinensis
KT232019 1 Ophiocordyceps sinensis
#16
AT-biased Cluster B
AB067741 1 Ophiocordyceps sinensis
AB067744 1 Ophiocordyceps sinensis
AJ786590 1 Ophiocordyceps sinensis
KC305892 1 Ophiocordyceps sinensis
AB067742 1 Ophiocordyceps sinensis
AB067748 1 Ophiocordyceps sinensis
AB067749 1 Ophiocordyceps sinensis
KP731800 1 Ophiocordyceps sinensis
KP731801 1 Ophiocordyceps sinensis
#4
AT-biased genotypes of Ophiocordyceps sinensis
KT232017 1 Ophiocordyceps sinensis
KT232018 1 Ophiocordyceps sinensis
#15
GC-biased genotypes of Ophiocordyceps sinensis
AB067721 1 Ophiocordyceps sinensis
AJ243776 1 Ophiocordyceps sinensis
AJ243980 1 Ophiocordyceps sinensis
HM135167 1 Ophiocordyceps sinensis
AJ488237 1 Ophiocordyceps sinensis
AJ488241 1 Ophiocordyceps sinensis
#1
AJ488254 1 Ophiocordyceps sinensis #7
ANOV01021709 1 Ophiocordyceps sinensis CO18 Genome sequence of H. sinensis strain Co18
EU570925 1 Ophiocordyceps sinensis
EU570929 1 Ophiocordyceps sinensis
EU570933 1 Ophiocordyceps sinensis
EU570956 1 Ophiocordyceps sinensis
EU570957 1 Ophiocordyceps sinensis
#1
JQ695935 1 Ophiocordyceps sinensis #11
HM595984 1 Ophiocordyceps sinensis
KJ175206 1 Ophiocordyceps sinensis
FJ654148 1 Ophiocordyceps sinensis
JQ325108 1 Ophiocordyceps sinensis
#3
GU246277 1 Ophiocordyceps sinensis #1
GU246280 1 Ophiocordyceps sinensis
GU246296 1 Ophiocordyceps sinensis
#12
GU246286 1 Ophiocordyceps sinensis #8
MG770309 1 Ophiocordyceps sinensis #2
GU246287 1 Ophiocordyceps sinensis #9
GU246291 1 Ophiocordyceps sinensis #12
GU246288 1 Ophiocordyceps sinensis #10
GU246290 1 Ophiocordyceps sinensis
HM769960 1 Ophiocordyceps sinensis
#1
JAAVMX010000019 1 Ophiocordyceps sinensis Genome sequence of H. sinensis strain IOZ07
JN049854 1 Ophiocordyceps sinensis
JQ325151 1 Ophiocordyceps sinensis
JQ900169 1 Ophiocordyceps sinensis
JX050171 1 Ophiocordyceps sinensis
JX402628 1 Ophiocordyceps sinensis
#1
LKHE01000582 1 Ophiocordyceps sinensis Genome sequence of H. sinensis strain 1229
LWBQ01000008 1 Ophiocordyceps sinensis Genome sequence of H. sinensis strain ZJB12195
NGJJ01000799 1 Ophiocordyceps sinensis Genome sequence of H. sinensis strain CC1406-203
KT339190 1 uncultured Ophiocordyceps sinensis #13
KT340698 1 Ophiocordyceps sinensis
AB067719 1 Ophiocordyceps sinensis
AB067719-type Group E fungus (outgroup control)
KT339178 1 uncultured Ophiocordyceps sinensis #14
AY986958 1 Ophiocordyceps sinensis
AY986956 1 Ophiocordyceps sinensis
AY986959 1 Ophiocordyceps sinensis
AB067719-type Group E fungus (outgroup control)
0.050

Fig 7. Bayesian phylogenetic analysis of multiple genotypes of *O. sinensis*. Five ITS sequences of the whole genomes (ANOV01021709, LKHE01000582, LWBQ01000008, JAAVMX010000002 and JAAVMX010000019) of *H. sinensis* strains (Co18, 1229, ZJB12195 and IOZ07) and 59 ITS sequences of 17 genotypes of *O. sinensis* were analyzed. The Bayesian majority-rule consensus tree was inferred using MrBayes v3.2.7a software (Markov chain Monte Carlo [MCMC] algorithm) [75]. GC-biased Genotypes #1–3 and #7–14 of *O. sinensis* are indicated in blue alongside the tree, and the AT-biased Genotypes #4–6 and #15–17 of *O. sinensis* are indicated in red alongside the tree. The AB067719-type Group-E sequences are indicated in purple alongside the tree as an outgroup control.

GC-biased genotypes of *O. sinensis* are indicated in blue alongside the tree in Fig 7, including Genotypes #1–3 and #8–14 and the ITS sequences from 5 whole-genome sequences of *H. sinensis* strains 1229, CC1406-203, Co18, IOZ07 and ZJB12195.

The AT-biased genotypes of *O. sinensis* are indicated in red alongside the tree and cluster into a clade that contains 2 branches. Cluster-A includes Genotypes #5–6 and #16–17, and Cluster-B includes Genotypes #4 and #15.

The AB067719-type Group-E fungus is side-noted in purple in Fig 7 as an outgroup control and is located outside of the blue GC-biased branch and the red AT-biased genotype clade.

Genotype #13 formed a phylogenetic leaf clustered close to the GC-biased branch. This leaf was distant from one of its parental fungi, Group-A Genotype #1 *H. sinensis*, but farther away from another parental fungus, the AB067719-type Group-E fungus.

Genotype #14 formed another phylogenetic leaf at a position closer to the parental AB067719-type Group-E fungus than to another parental fungus, Group-A Genotype #1 *H. sinensis*.

GC-biased Genotype #1 and AT-biased Genotypes #5–6 and #16, as well as *S. hepiali* and the AB067719-type fungus, were detected in the ascospores of *C. sinensis*. Genotypes #5–6 and #16 were located within AT-biased Cluster-A in the Bayesian tree (Fig 7). Genotypes #4 and #15 form AT-biased Cluster-B in the Bayesian tree and were detected in the stroma and SFP (with ascocarps) but not in the ascospores of *C. sinensis* (*cf*. Table 2, Fig 7).

Discussion

Differential occurrence of multiple genotypes of *O. sinensis* and dynamic

alterations of the genotypes during *C. sinensis* maturation

In addition to the 12 *O. sinensis* genotypes previously discovered [15–16,18,24,27–28,31–34,50,57–60,66], the current study identified 5 new genotypes of *O. sinensis*: AT-biased Genotypes #15–17 with multiple transition point mutations and GC-biased Genotypes #13–14 that exhibit the characteristics of large DNA segment reciprocal substitutions and genetic material recombination in natural *C. sinensis*. These genotypes occurred differentially in the stroma, SFP (with ascocarps), and 2 types of ascospores of *C. sinensis (cf.* Table 2). The biomasses of the GC- and AT-biased genotypes undergo dynamic alterations in an asynchronous, disproportional manner during *C. sinensis* maturation, as demonstrated using a Southern blotting approach without DNA amplification [18,27].

The ITS sequences of Genotype #1 were the most easily amplifiable and detectable using universal primers, but this finding may not necessarily imply dominance of the Genotype #1 DNA template in the test samples [7]. Southern blotting analysis without DNA amplification demonstrated that AT-biased genotypes were dominant in the stroma of natural *C. sinensis* during maturation, and GC-biased Genotype #1 was never the dominant fungus in the stroma [27–28]. The easy pairing and elongation of the Genotype #1 ITS sequences using universal primers were observed due to (1) the sequence identity levels and (2) the absence of secondary structure/conformation in their sequences that could interfere with PCR amplification and sequencing [7]. In early molecular studies on *C. sinensis* (1999–2006), mycologists reported the detection of a single sequence of *H. sinensis* and therefore incorrectly judged *H. sinensis* to be the sole anamorph of *O. sinensis*.

Chen et al. [36] first reported the molecular heterogeneity of *C. sinensis*-associated fungi of the genera *Hirsutella*, *Paecilomyces* and *Tolypocladium* using a PCR amplicon cloning-sequencing methodology. However, insufficient attention was given to the "all-or-none" qualitative research technique and findings, and instead, the disproportionate amplicon clones selected for examination of the ITS sequences of different fungi were overemphasized, which unfortunately led to the improper conclusion that *H. sinensis* was the sole anamorph of *O. sinensis*. As demonstrated herein, we applied multiple pairs of genotype- and species-specific primers and cloning-based amplicon sequencing approaches with selection of at least 30 white colonies per Petri dish in cloning experiments, which enabled us to profile the components of the heterogeneous metagenome in the immature and mature stromata, SFP (with ascocarps), and ascospores of natural *C. sinensis*. In particular, this approach allowed us to identify those genotypes and fungi with low abundance and those with secondary structure/conformation in their DNA

509 sequences, which may affect primer binding and DNA chain elongation during PCR amplification and
510 sequencing [7–10].

511 GC-biased Genotypes #1 and #2 coexisted in the stroma of natural *C. sinensis*, and their amplicon
512 abundance was low in the immature stroma (1.0–2.0 cm in stromal height) [27–28]. Genotype #1 showed
513 a greatly elevated abundance in the maturing stroma (4.0–4.5 cm in height without an expanded fertile
514 portion close to the stromal tip), and its abundance then plateaued in the mature stroma (6.5–7.0 cm in
515 height, showing the formation of an expanded fertile portion close to the stromal tip, which is densely
516 covered with ascocarps) (Fig 8; modified from Fig 6 of [28] in Chinese). In contrast to the maturation
517 pattern of Genotype #1, the abundance of Genotype #2 remained at a low level in the maturing stroma and
518 increased markedly in the mature stroma to a level that exceeded the abundance of Genotype #1. The
519 cooccurrence of Genotypes #1 and #2 in the stroma with distinct maturation patterns indicates the genomic
520 independence of the 2 GC-biased genotypes, which is proven by the absence of Genotype #2 sequences
521 in the whole-genome sequences of 5 Genotype #1 *H. sinensis* strains [7–12,30–31,51–55].

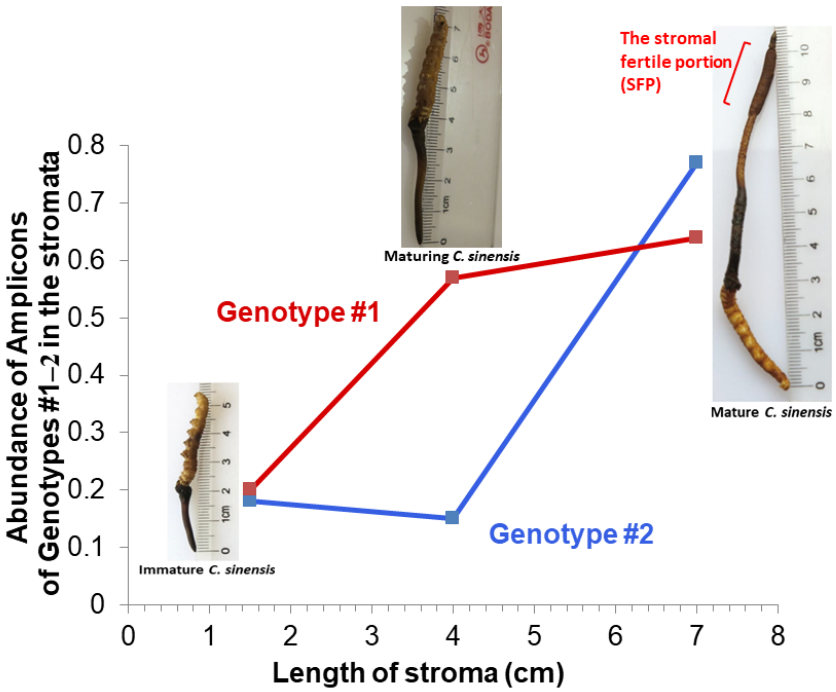

522

523 **Fig 8. Dynamic alterations of the abundance of the amplicons of Genotypes #1 and #2 of *O. sinensis* in the**
524 **stromata of *C. sinensis* during maturation (modified from Fig 6 of [28]).** Immature *C. sinensis* had very short
525 stroma of 1.5 cm. Maturing *C. sinensis* had stroma of 4.0 cm without an expanded fertile portion close to the
526 stroma tip. Mature *C. sinensis* had long stroma of 7.0 cm and showed the formation of an expanded fertile portion
527 close to the stroma tip, which was densely covered with ascocarps.

528 In this study, we did not detect GC-biased Genotypes #3 and #7–12 of *O. sinensis* in the
529 compartments of natural *C. sinensis* specimens collected from the Hualong and Yushu areas of Qinghai
530 Province. This may indicate that these GC-biased genotypes of *O. sinensis* may exist in the natural *C.*
531 *sinensis* specimens in different production areas.

532 A Bayesian phylogenetic analysis (*cf.* Fig 7) demonstrated that the AT-biased genotypes were
533 clustered into 2 branches, Clusters A and B. AT-biased genotypes from both branches were detected in
534 the stroma and SFP of *C. sinensis*, but Genotypes #4 and #15 of Cluster-B were absent in the ascospores,
535 consistent with those discovered by Li et al. [61]. Genotype #4 of AT-biased Cluster-B was the dominant
536 AT-biased genotype in the immature stroma during the asexual growth stage and coexisted with less
537 dominant Genotypes #5–6 of AT-biased Cluster-A [16–17]. The abundance of Genotype #4 of Cluster-B
538 markedly decreased in the mature *C. sinensis* stroma and remained at a low level in the SFP (with
539 ascocarps) during the sexual growth stage. In contrast, the abundance of Genotype #5 of AT-biased
540 Cluster-A increased reciprocally and significantly in the mature *C. sinensis* stroma and SFP and
541 predominated in the *O. sinensis* ascospores [16–17,69]. In addition, Genotype #15 of Cluster-B
542 predominated in the SFP (with ascocarps) of *C. sinensis* prior to ascospore ejection and drastically
543 declined after ejection [69]. The differential cooccurrence and alternative predominance of GC- and AT-
544 biased genotypes of *O. sinensis* indicate their distinct physiological functions at different maturational
545 stages of the *C. sinensis* lifecycle and their genomic independence, belonging to independent *O. sinensis*
546 fungi.

547 Engh [32], Kinjo & Zang [34], Wei et al. [50] and Mao et al. [59] reported the detection of either
548 Genotype #4 or #5 of *O. sinensis*, without codetection of GC-biased Genotype #1 *O. sinensis*, in some
549 natural *C. sinensis* specimens collected from geographically distant areas and in cultivated *C. sinensis*.
550 These findings likely indicate that the studied specimens might be in different maturational stages and that
551 the amplicons of other cocolonized *O. sinensis* genotypes and fungal species might be overlooked during
552 PCR amplification and sequencing due to lower-abundance amplicons caused by the experimental designs
553 without using genotype- and species-specific primers or cloning-based amplicon sequencing strategies or
554 due to secondary structures present in the sequences of *O. sinensis* genotypes, which may interfere with
555 primer binding, DNA chain elongation, and sequencing [7].

556 In this study, we detected several AT-biased genotypes of Cluster-A and GC-biased Genotypes #1
557 *H. sinensis* and #13–14 in ascospores that cooccurred with *S. hepiali* and the AB067719-type fungus in
558 the teleomorphic ascospores of natural *C. sinensis*. However, AT-biased Cluster-B genotypes were absent

559 in ascospores but present in the SFP (with ascocarps). *Pseudogymnoascus roseus*, *Geomyces pannorum*,
560 *Tolypocladium sinensis*, and *Penicillium chrysogenum* were not detected in the SFP (with ascocarps) and
561 ascospores of *C. sinensis* despite their differential predominance in the stroma and caterpillar body of
562 natural *C. sinensis* found in 2 previous mycobiota studies [40–41].

563 The sequences of Genotypes #2–17 of *O. sinensis*, however, were not present in the genome
564 assemblies (ANOV00000000, JAAVMX000000000, LKHE00000000, LWBQ00000000 and
565 NGJJ00000000) of 5 Genotype #1 *H. sinensis* strains, Co18, IOZ07, 1229, ZJB12195 and CC1406-203,
566 and instead belonged to the genomes of independent *O. sinensis* fungi [7–12,27–28,30–31,51–56,69].
567 These genomic independence findings support the hypotheses of independent *O. sinensis* fungi and an
568 integrated microecosystem for natural *C. sinensis* [14,24]. During the complex lifecycle of natural *C.*
569 *sinensis*, its metagenomic members appear to function mutually and symbiotically at different
570 development-maturation stages in a dynamically alternating manner from the immature to the maturing
571 and then the mature stages and from initial asexual growth to sexual growth and reproduction.

572

573 Complex anamorph-teleomorph connection of *O. sinensis*

574 The anamorph-teleomorph connection of *O. sinensis* has been the subject of decades-long academic
575 debate [7–12,29,62]. Wei et al. [44] hypothesized that *H. sinensis* is the sole anamorph of *O. sinensis*
576 based on the 3 aforementioned sets of evidence; this hypothesis satisfied the requirements of the first and
577 second criteria of Koch's postulates, but unfortunately not the third and fourth criteria, making the
578 hypothesis uncertain [7–12,29–31,56]. Although this hypothesis has been widely appreciated, Wei et al.
579 [44] demonstrated significant genetic diversity of *O. sinensis* teleomorphs (*cf.* the far phylogenetic
580 distance with a low bootstrap value between those of natural *C. sinensis* specimens G3 and S4, shown in
581 Fig 6 of [44]).

582 Bushley et al. [76] discovered the multicellular heterokaryotic structure of the hyphae and
583 ascospores of *C. sinensis*, which contain multiple mononucleated, binucleated and trinucleated cells. Li et
584 al. [61], the research partners in the study [76], reported the identification of both GC-biased Genotype #1
585 and AT-biased Genotype #5 in 8 of 15 clones derived from the 25-day culture of a *C. sinensis* mono-
586 ascospore. Based on insufficient and contradictory evidence, these researchers overinterpreted that all AT-
587 biased genotypes were "ITS pseudogene" components of the genome of Genotype #1 *H. sinensis*, in
588 agreement with the sole anamorph hypothesis for *H. sinensis* [44]. However, AT-biased genotype

589 sequences are not present in the 5 whole-genome assemblies (ANOV0000000, JAAVMX0000000000,
590 LKHE00000000, LWBQ00000000 and NGJJ00000000) of Genotype #1 *H. sinensis* strains Co18, IOZ07,
591 1229, ZJB12195 and CC1406-203 [7–10,31,51–55]. The genomic independence evidence disproved the
592 "ITS pseudogene" hypothesis for the AT-biased genotypes of *O. sinensis* proposed by Li et al. [61].

593 In contrast, Barseghyan et al. [74] proposed a dual-anamorph hypothesis for *O. sinensis* involving
594 *Tolypocladium sinensis* and *H. sinensis* using macro- and micromycological approaches, but it leaves an
595 unresolved question regarding the genotype of *O. sinensis* with *H. sinensis*-like morphological and growth
596 characteristics. Engh [32] hypothesized that *C. sinensis* and *T. sinensis* form a fungal complex in the
597 natural insect-fungal complex, and the *C. sinensis* sequence AJ786590 was disclosed and uploaded to the
598 GenBank database by Stensrud et al. [65]. Stensrud et al. [66] clustered AJ786590 and other sequences
599 into Group-B of *O. sinensis* using a Bayesian phylogenetic approach and concluded that Group-B (AT-
600 biased Genotype #4) sequences are phylogenetically distinct from GC-biased Group-A of *O. sinensis*
601 (Genotype #1 *H. sinensis*).

602 Kinjo & Zang [34], Engh [32], Wei et al. [50] and Mao et al. [59] detected AT-biased Genotype #4
603 or #5 of *O. sinensis* from natural *C. sinensis* specimens collected from different geographic regions or
604 from cultivated *C. sinensis*. Zhang et al. [57] and Cheng et al. [58] reported the detection of GC-biased
605 Genotype #3 of *O. sinensis* in natural *C. sinensis* collected from Nyingchi in Tibet. Chen et al. [60]
606 reported the detection of GC-biased Genotype #7 of *O. sinensis* from the stroma of *C. sinensis* specimens
607 collected from Qinghai Province of China. These mutant genotypes of *O. sinensis* share the same *H.*
608 *sinensis*-like morphological and growth characteristics without the cooccurrence of Genotype #1 *H.*
609 *sinensis*, although they may share a common evolutionary ancestor [32,34,57–60,66]. In the current study,
610 we detected AT-biased Cluster-A genotypes (*cf*. Fig 7) and GC-biased Genotypes #1 and #13–14 in the
611 teleomorphic ascospores of *C. sinensis*, along with *S. hepiali* and the AB067719-type fungus, and
612 additional AT-biased Cluster-B genotypes in the stroma and SFP (with ascocarps) of *C. sinensis*.

613 Li et al. [43] recently reported the differential occurrence and transcription of the mating-type genes
614 of the *MAT1-1* and *MAT1-2* idiomorphs in 237 *H. sinensis* strains, indicating genetic and transcriptional
615 inability to perform self-fertilization under homothallic or pseudohomothallic reproduction, as proposed
616 by Hu et al. [51] and Bushley et al. [76]. Although Bushley et al. [76] reported the transcription of both
617 the MAT1-1-1 and MAT1-2-1 genes of the *MAT1-1* and *MAT1-2* idiomorphs, the MAT1-2-1 transcript of
618 *H. sinensis* strain 1229 harbored unspliced intron I, which contains 3 stop codons. This type of transcript
619 presumably produces a truncated and dysfunctional MAT1-2-1 protein missing the majority portion of the

620 protein encoded by exons II and III [43,78]. These findings constitute a coupled transcriptional-
621 translational mechanism of *H. sinensis* reproductive control, in addition to the controls at the genetic and
622 transcriptional levels. The differential occurrence and transcription of the mating genes of the *MAT1-1* and
623 *MAT1-2* idiomorphs indicate that *H. sinensis* requires a sexual partner to perform physiologically
624 heterothallic reproduction in the lifecycle of natural *C. sinensis* regardless of whether *H. sinensis* is
625 monoecious or dioecious [43,78]. For example, *H. sinensis* strains 1229 and L0106 appear to reciprocally
626 produce functional MAT1-1-1 and MAT1-2-1 transcripts and presumably complementary mating proteins
627 [76,79], possibly constituting a pair of sexual partners for physiological heterothallism [43,78]. In addition,
628 the transcripts of mating-type genes in *S. hepiali* strain Feng [80] were coincidentally found to be
629 complementary to those of *H. sinensis* strain L0106 [79]. The coincident transcriptomic findings reveal a
630 possible transcriptomic mechanism for fungal hybridization, which triggers further investigation because
631 *H. sinensis* is closely associated with a small quantity of *S. hepiali* in the compartments of natural *C.*
632 *sinensis*, often resulting in difficulties in fungal isolation and purification even by top-notch mycology
633 taxonomists [77].

634 Wei et al. [50] reported an industrial artificial cultivation project in which 3 anamorphic *H. sinensis*
635 strains, 130508-KD-2B, 20110514 and H01-20140924-03, were reportedly used as inoculants. The
636 successful cultivation of *C. sinensis* is important for supplementing the increasingly scarce natural
637 resources of *C. sinensis* and for meeting the third criterion of Koch's postulates, adding academic value
638 to supplement the 3 aforementioned sets of evidence [44]. However, these authors reported the
639 identification of the sole teleomorph of *O. sinensis* in the fruiting body of cultivated *C. sinensis*, and it
640 belonged to AT-biased Genotype #4. Thus, the apparent fungal mismatch between the inoculants used in
641 artificial cultivation and the final cultivated product resulted in failure to meet the requirement of the
642 fourth criterion of Koch's postulates. In addition to the detection of teleomorphic AT-biased Genotype #4
643 in cultivated *C. sinensis*, Wei et al. [50] also reported the detection of teleomorphic GC-biased Genotype
644 #1 in natural *C. sinensis*. Because the sequence of AT-biased Genotype #4 is absent in the 5 whole-genome
645 assemblies (ANOV00000000, JAAVMX000000000, LKHE00000000, LWBQ00000000 and
646 NGJJ00000000) of the GC-biased Genotype #1 *H. sinensis* strains Co18, IOZ07, 1229, ZJB12195 and
647 CC1406-203 [51–55], the scientific evidence reported by Wei et al. [50] disproves the sole anamorph and
648 sole teleomorph hypotheses for *O. sinensis*, which were proposed 10 years ago by the same group of key
649 authors [44]. The species mismatch reported by Wei et al. [50] may imply (1) that the researchers could
650 have overlooked the Genotype #4 sequence in one or all of the anamorphic inoculant strains, which would

651 confirm previous findings that GC-biased Genotype #1 *H. sinensis* (Group-A) and AT-biased genotypes
652 (Groups B and C) formed a species complex [66] and that the actual causative agent is a fungal (species)
653 complex containing several *O. sinensis* genotypes and *S. hepiali* [77]; or (2) that secondary or sequential
654 infections by the true causal fungus/fungi (Genotype #4 and possibly other genotypes of *O. sinensis*)
655 occurred in the course of artificial cultivation. A third possibility is that a series of preprogrammed,
656 nonrandom mutagenic conversions of GC-biased Genotype #1 to AT-biased Genotype #4 occurred during
657 artificial cultivation without exception in all cultivated *C. sinensis* products (and *vice versa* after the
658 ejection of the ascospores); however, this possibility seems the least likely.

659 Zhang et al. [81] summarized nearly 40 years of artificial cultivation experience with failed
660 induction of fruiting body and ascospore production in research-oriented academic settings, either in
661 fungal cultures or after infecting insects with fungal inoculants. Distinct from the success of artificial *C.*
662 *sinensis* cultivation in product-oriented industrial settings, as reported by Wei et al. [50], Hu et al. [51]
663 inoculated 40 larvae of *Hepialus* sp. with 2 pure *H. sinensis* strains (Co18 and QH195-2) *via* the injection
664 of a mycelial mixture through the second larval proleg, which caused death and mummification of the
665 larvae but failed to induce the production of a fruiting body. Li et al. [77] inoculated 400 larvae of *Hepialus*
666 *armoricanus* with 4 groups of inoculants (n=100 larvae per inoculant): (1) conidia of *H. sinensis*, (2)
667 mycelia of *H. sinensis*, (3) purified ascospores of *C. sinensis*, and (4) a mixture of 2 wild-type fungal
668 strains, CH1 and CH2, isolated from the intestines of healthy living larvae of *Hepialus lagii* Yan [82].
669 Both strains CH1 and CH2 showed *H. sinensis*-like morphological and growth characteristics and
670 contained GC-biased Genotype #1 *H. sinensis* and *S. hepiali* as well as highly abundant AT-biased
671 Genotype #5 of *O. sinensis* and the markedly less abundant Genotypes #4 and #6 [77]. The application of
672 a mycelial mixture of strains CH1 and CH2 as the inoculant resulted in a favorable infection-mortality-
673 mummification rate of 55.2±4.4%, indicating 15–39-fold greater potency than the infection-mortality-
674 mummification rates (1.4–3.5%; $P<0.001$) achieved after inoculation with the conidia or mycelia of *H.*
675 *sinensis* or ascospores of *C. sinensis*. These findings reported by Li et al. [43,77], Wei et al. [50], Hu et al.
676 [51], and Zhang et al. [81] suggest that GC-biased Genotype #1 *H. sinensis* may not be the sole true
677 causative fungus in natural *C. sinensis* and that inoculation synergy of the symbiotic fungal species may
678 be needed to initiate the development of the stromal primordia and fruiting bodies, and sexual partners,
679 regardless of whether they are the same or interspecific species, may be needed to induce the transition
680 from asexual to sexual growth and reproduction and the maturation of the teleomorphic ascocarps and
681 ascospores during the lifecycle of natural and cultivated *C. sinensis*.

682 The microcycle conidiation of *C. sinensis* ascospores using culture protocols favoring the growth of
683 *H. sinensis* has also been reported [45–47]. Bushley et al. [76] demonstrated that *C. sinensis* ascospores
684 are multicellular and heterokaryotic, consisting of multiple monokaryotic, bikaryotic and trikaryotic cells.
685 Our study herein demonstrated that the fully ejected *C. sinensis* ascospores contain GC-biased Genotypes
686 #1 and #14, AT-biased Genotypes #5–6 and #16 within AT-biased Cluster-A, *S. hepiali* and the
687 AB067719-type fungus (*cf.* Table 2 and Fig 7). These findings suggest a multicellular heterokaryotic
688 structure and genetic heterogeneity of ascospores [7–10]. However, the culture-dependent approach
689 detected only GC-biased Genotype #1 and AT-biased Genotype #5 after 25-day liquid inoculation of
690 mono-ascospores [61], suggesting the possibility of overlooking several AT-biased genotypes and GC-
691 biased Genotypes #14, probably due to nonculturability of those genotypes or inappropriately designed
692 and executed molecular techniques. The nonculturable nature of most genotypes of *O. sinensis* fungi
693 examined to date [62–64] calls into question whether all genotypes of *O. sinensis* in all cells of
694 multicellular heterokaryotic ascospores are capable of undergoing conidiation through *in vitro* microcycle
695 conidiation under the commonly used experimental conditions that favor the growth of Genotype #1 *H.*
696 *sinensis*. The lack of molecular information on conidia in these studies [45–47] makes the
697 fungal/genotypic identity of the conidia uncertain due to the *H. sinensis*-like morphological and growth
698 characteristics shared by multiple genotypes of *O. sinensis* [32,34,50,57–61,76–77] and the *Hirsutella*-
699 like morphology shared by numerous fungal species in the families Ophiocordycipitaceae and
700 Clavicipitaceae and the genera *Polycephalomyces* and *Harposporium* [83].

701 The study described herein further revealed fungal and genotypic heterogeneity in the multicellular
702 heterokaryotic ascospores of *C. sinensis*. AT-biased Cluster-A genotypes, GC-biased Genotype #1 *H.*
703 *sinensis* and Genotypes #13 or #14 (showing large DNA segment reciprocal substitutions and genetic
704 material recombination) in either type of ascospores, *S. hepiali* and the AB067719-type Group-E fungus
705 naturally cooccur in teleomorphic *C. sinensis* ascospores.

706

707 Differential occurrence of Genotypes #4 and #15 of AT-biased Cluster-B

708 Studies of natural and cultivated *C. sinensis* have detected Genotype #4 of *O. sinensis*, but not
709 coexisting GC- and AT-biased genotypes of *O. sinensis*, including AJ786590 discovered by Engh [32]
710 and uploaded to GenBank by Stensrud et al. [65], AB067741–AB067749 identified by Kinjo & Zang [34],
711 KC305891–KC305892 discovered by Mao et al. [59], and 2 sequences ("Fruiting body 3" and "Mycelia

712 3", sequences unavailable in GenBank) with high homology to AB067749 and KC305892 found by Wei
713 et al. [50]. These studies did not report the maturation stages of natural and cultivated *C. sinensis*
714 specimens that were used as the study materials. However, other studies using genotype-specific primers,
715 amplicon cloning and biochip-based SNP mass spectrometry genotyping techniques reported the detection
716 of Genotype #4 of *O. sinensis* in natural *C. sinensis* coexisting with Genotype #1 *H. sinensis* with or
717 without Genotypes #5–6 [16–18,24,27–28,61,69].

718 Genotype #4 of AT-biased Cluster-B was found to predominate in the stroma of immature *C.*
719 *sinensis* and to decline during *C. sinensis* maturation (*cf*. Fig 7) [16–17,27–28,30–31,69]. Genotype #4
720 and the newly discovered Genotype #15 of AT-biased Cluster-B are present in the SFP (with ascocarps)
721 but not in ascospores of natural *C. sinensis* (*cf*. Table 2) [69].

722

723 Fungal factors involved in the control of the development, maturation and 724 ejection of *C. sinensis* ascospores

725 In this study, we report the discovery of 2 types of ascospores of *C. sinensis*, namely, fully and
726 semiejected ascospores. In contrast to the well-described fully ejected ascospores, semiejected ascospores
727 show tight adhesion to the outer surface of asci, hanging out of the perithecial opening (*cf*. lower-right
728 panel of Fig 1, Figs 4B and 4E). The distinct ejection behaviors of ascospores are associated with divergent
729 fungal compositions. In addition to the cooccurrence of GC-biased Genotype #1, AT-biased Cluster-A
730 genotypes and the AB067719-type fungus in the 2 types of ascospores, the semiejected ascospores contain
731 Genotype #13 of *O. sinensis* and a greater abundance of *S. hepiali*, whereas the fully ejected ascospores
732 contain Genotype #14 and a markedly lower abundance of *S. hepiali (cf*. Fig 5 and Table 2). Genotypes
733 #13–14 show alternating reciprocal substitutions of large DNA segments between the genomes of 2
734 parental fungi, namely, Genotype #1 *H. sinensis* (Group-A by [66]) and the AB067719-type Group-E
735 fungus (*cf*. Table 3 and Fig 6), indicating that the biological processes of plasmogamy, karyogamy,
736 chromosomal intertwining interaction, and genetic material recombination occur differentially between
737 the 2 parental fungi regardless of the processes of hereditary variation caused by fungal hybridization or
738 parasexual reproduction [9,43]. The divergent fungal components with altered abundances may participate
739 in the control of the development, maturation and ejection of *C. sinensis* ascospores.

740 Genotypes #6 and #16 of AT-biased Cluster-A were detected in fully ejected ascospores but not in

741 semiejected ascospores using genotype-specific primers and cloning-based amplicon sequencing (*cf.*
742 Tables 2; Fig 7). The differential occurrence of these 2 AT-biased genotypes may need to be further
743 verified due to the possible existence of secondary structures/conformation in the DNA sequences that
744 may affect primer binding and DNA chain elongation during PCR amplification and sequencing [7–10].
745 In fact, Genotypes #6 and #16 were detected in both types of ascospores using the biochip-based
746 MassARRAY SNP mass spectrometry technique [69].

747

748

749 # Conclusions

750 This study identified 2 types of multicellular heterokaryotic ascospores collected from the same
751 natural *C. sinensis* specimens. Multiple genotypes of *O. sinensis* coexist differentially in the 2 types of *C.*
752 *sinensis* ascospores and are accompanied by *S. hepiali* and the AB067719-type fungus. The divergent
753 fungal components of the 2 types of ascospores may participate in the control of the development,
754 maturation and ejection of the ascospores. The AT-biased Cluster-A genotypes are present in the stroma,
755 SFP (with ascocarps), and ascospores; however, the AT-biased Cluster-B genotypes are present in the
756 stroma and SFP but not in ascospores. Multiple fungal components occur differentially in the
757 compartments of natural *C. sinensis* and undergo dynamic alterations in an asynchronous, disproportional
758 manner during *C. sinensis* maturation. These findings describe part of the complex lifecycle of this
759 precious TCM therapeutic agent whose metagenomic components undergo dynamic alterations at different
760 development and maturation stages in a symbiotic manner.

761

762

763 # Acknowledgments

764 The authors are grateful to Prof. Mu Zang, Prof. Ru-Qin Dai, Prof. Ying-Lan Guo, Prof. Ping Zhu,
765 Prof. Zong-Qi Liang, Prof. Zhao-Lan Li, Prof. Yu-Guo Zheng, Dr. Jia-Gang Zhao and Dr. Yan-Jiao Zhou
766 for consultations and Prof. Xin Liu, Prof. Hai-Feng Xu, Ms. Xiao-Li Ma, Ms. Ming Yang, Mr. Zong-Hao
767 Zhang, Mr. Wei Chen, Mr. Tao-Ye Zheng, Mr. Jin-Jin Li, and Mr. Yu-Chun Zhou for their assistance.

768

769

770 # References

771 [1] Song L-R, Hong X, Ding X-L, Zang Z-Y. *Monographs of Modern Pharmacy of Chinese*
772 *Traditional Medicine*. 1st ed. People′s Health Publishing House, Beijing 2001. pp. 733–737.

773 [2] Zhu J-S, Halpern GM, Jones K. The scientific rediscovery of a precious ancient Chinese herbal
774 regimen: *Cordyceps sinensis*: Part I. J Altern Complem Med. 1998a;4(3): 289–303.

775 [3] Zhu J-S, Halpern GM, Jones K. The scientific rediscovery of an ancient Chinese herbal medicine:
776 *Cordyceps sinensis*: Part II. J Altern Complem Med. 1998b;4(4): 429–457.

777 [4] Lo H-C, Hsieh C, Lin F-Y, Hsu T-H. A Systematic Review of the Mysterious Caterpillar Fungus
778 *Ophiocordyceps sinensis* in Dōng Chóng Xià Cǎo and Related Bioactive Ingredients. J Tradit
779 Compliment Med. 2013;3(1): 16-32.

780 [5] Zhu J-S, Li C-L, Tan N-Z, Berger JL, Prolla TA. Combined use of whole-gene expression profiling
781 technology and mouse lifespan test in anti-aging herbal product study. Proc. 2011 New TCM Prod.
782 Innovat. Indust. Devel. Summit, Hangzhou, China, 2011. pp. 443–448. Available from
783 https://xueshu.baidu.com/usercenter/paper/show?paperid=08341c17fa58c8f85584b92572b90f75

784 [6] Tan N-Z, Berger JL, Zhang Y, Prolla TA, Weindruch R, Zhao C-S, et al. The lifespan-prolonging
785 effect of *Cordyceps sinensis* Cs-4 in normal mice and its molecular mechanisms. FASEB J.
786 2011;25(1): 599.1. https://doi.org/10.1096/fasebj.25.1_supplement.599.1

787 [7] Zhu J-S, Wu J-Y. Genetic heterogeneity of natural *Cordyceps sinensis* with co-existence of
788 multiple fungi. Chin J Cell Biol. 2015;37(2): 284–298.

789 [8] Zhu J-S, Li Y-L. A Precious Transitional Chinese Medicine, *Cordyceps sinensis*: Multiple
790 heterogeneous *Ophiocordyceps sinensis* in the insect-fungi complex. 1st ed. Lambert Academic
791 Publishing, Saarbrüchen. Germany 2017. Available from https://www.amazon.com/Precious-
792 Traditional-Medicine-Cordyceps-sinensis/dp/3330046686

793 [9] Li Y-L, Li X-Z, Zhu J-S. *Cordyceps sinensis* Fungal Heterokaryons. 1st ed. Chemistry Industry
794 Press Co., Beijing, China, 2022. Available from https://www.cip.com.cn/Book/Index/48939

795 [10] Li Y-L, Yao Y-S, Xie W-D, Zhu J-S. Molecular heterogeneity of natural *Cordyceps sinensis* with
796 multiple *Ophiocordyceps sinensis* fungi challenges the anamorph-teleomorph connection
797 hypotheses and implementation of the Amsterdam Declaration of IMA. Am J Biomed Sci.
798 2016;8(2): 123−159.

799 [11] Yao Y-S, Zhu J-S. Indiscriminative use of the Latin name for natural *Cordyceps sinensis* insect-
800 fungi complex and multiple *Ophiocordyceps sinensis* fungi. Chin J Chin Mater Med. 2016;41(7):
801 1361–1366.

802 [12] Li X-Z, Li Y-L, Yao Y-S, Xie W-D, Zhu J-S. Molecular identification of *Ophiocordyceps sinensis*
803 genotypes and the indiscriminate use of the Latin name for the multiple genotypes and the natural
804 insect-fungi complex. Am J Biomed Sci. 2022;14(3): 115–135.

805 [13] Xu J-T. Chinese Medicinal Mycology. Beijing Med. Univ. Press and China Peking Union Med.
806 Univ. Press, Beijing, 1997. pp. 354–385. http://product.dangdang.com/1836661907.html

807 [14] Liang Z-Q, Han Y-F, Liang J-D, Dong X, Du W. Issues of concern in the studies of
808 *Ophiocordyceps sinensis*. Microbiol Chin. 2010;37(11): 1692–1697.

809 [15] Zhang W-W, Cheng X-L, Liu X-Z, Xiang M-C. Genome Studies on Nematophagous and
810 Entomogenous Fungi in China. J Fungi. 2016;2: 9. doi:10.3390/jof2010009

811 [16] Gao L, Li X-H, Zhao J-Q, Lu J-H, Zhu J-S. Detection of multiple *Ophiocordyceps sinensis*
812 mutants in premature stroma of *Cordyceps sinensis* by MassARRAY SNP MALDI-TOF mass
813 spectrum genotyping. J Peking Univ (Health Sci). 2011;43(2): 259–266.

814 [17] Gao L, Li X-H, Zhao J-Q, Lu J-H, Zhao J-G, Zhu J-S. Maturation of *Cordyceps sinensis* associates
815 with alterations of fungal expressions of multiple *Ophiocordyceps sinensis* mutants with transition
816 and transversion point mutations in stroma of *Cordyceps sinensis*. J Peking Univ (Health Sci).
817 2012;44(3): 454–463.

818 [18] Yao Y-S, Zhou Y-J, Gao L, Lu J-H, Zhu J-S. Dynamic alterations of the differential fungal
819 expressions of *Ophiocordyceps sinensis* and its mutant genotypes in stroma and caterpillar during
820 maturation of natural *Cordyceps sinensis*. J Fungal Res. 2011;9(1): 37–49,53.

821 [19] Yao Y-S, Gao L, Li Y-L, Ma S-L, Wu Z-M, Tan N-Z, et al. Amplicon density-weighted algorithms
822 analyze dissimilarity and dynamic alterations of RAPD polymorphisms in the integrated micro-
823 ecosystem *Cordyceps sinensis*. J Peking Univ (Health Sci). 2014;46(4): 618–628.

824 [20] Dong Y-Z, Zhang L-J, Wu Z-M, Gao L, Yao Y-S, Tan N-Z, et al. Altered proteomic polymorphisms
825 in the caterpillar body and stroma of natural *Cordyceps sinensis* during maturation. PLoS ONE.
826 2014;9(10): e109083. doi: 10.1371/journal.pone.0109083

827 [21] Ni L-Q, Yao Y-S, Gao L, Wu Z-M, Tan N-Z, Wu J-Y, et al. Density-weighted algorithms for
828 similarity computation and cluster tree construction in the RAPD analysis of a micro-ecosystem

829 *Cordyceps sinensis*. Am J Biomed Sci. 2014;6(2): 82–104.

830 [22] Liu Y-N, Jin Y-S, Liu Z, Han Y-N. *Cordyceps sinensis* cDNA library construction and
831 identification. Chin J Informat TCM. 2006;13(9): 43−45.

832 [23] Yang J-L, Xiao W, He H-H, Zhu H-X, Wang S-F, Cheng K-D, et al. Molecular phylogenetic
833 analysis of *Paecilomyces hepiali* and *Cordyceps sinensis*. Acta Pharmaceut Sinica. 2008;43(4):
834 421–426.

835 [24] Xiao W, Yang J-P, Zhu P, Cheng K-D, He H-X, Zhu H-X, et al. Non-support of species complex
836 hypothesis of *Cordyceps sinensis* by targeted rDNA-ITS sequence analysis. Mycosystema.
837 2009;28(6): 724–730.

838 [25] Xiao Y-Y, Cao Y-M, Zhang L, Li C-R. Study on Genetic Diversity of Anamorphic Isolates from
839 Different Sources of *Ophiocordyceps sinensis* by ISSR. J Fungal Res. 2014;12(3): 154–159.

840 [26] Zhu J-S, Guo Y-L, Yao Y-S, Zhou Y-J, Lu J-H, Qi Y, et al. Maturation of *Cordyceps sinensis*
841 associates with co-existence of *Hirsutella sinensis* and *Paecilomyces hepiali* DNA and dynamic
842 changes in fungal competitive proliferation predominance and chemical profiles. J Fungal Res.
843 2007;5(4): 214–224.

844 [27] Zhu J-S, Gao L, Li X-H, Yao Y-S, Zhou Y-J, Zhao J-Q, et al. Maturational alterations of oppositely
845 orientated rDNA and differential proliferations of CG:AT-biased genotypes of *Cordyceps sinensis*
846 fungi and *Paecilomyces hepiali* in natural *C. sinensis*. Am. J. Biomed. Sci. 2010;2(3): 217–238.

847 [28] Zhu J-S, Zhao J-G, Gao L, Li X-H, Zhao J-Q, Lu J-H. Dynamically altered expressions of at least
848 6 *Ophiocordyceps sinensis* mutants in the stroma of *Cordyceps sinensis*. J. Fungal Res.
849 2012;10(2): 100–112.

850 [29] Jiang Y, Yao Y-J. A review for the debating studies on the anamorph of *Cordyceps sinensis*.
851 Mycosistema. 2003;22(1): 161–176.

852 [30] Zhu J-S, Li Y-L, Yao Y-S, Xie W-D. Molecular evidence not supporting the use of *Hirsutella*
853 *sinensis* strain EFCC7287 as the taxonomic standard for multiple *Ophiocordyceps sinensis* fungi.
854 Intl. J. Mol. Biol. 2018;3: 114−115.

855 [31] Zhu J-S, Li Y-L, Yao Y-S, Xie W-D. The multiple genotypes of *Ophiocordyceps sinensis* and the
856 "ITS pseudogene" hypothesis. Mol. Phylogenet Evol. 2019;139: 106322. doi:
857 10.1016/j.ympev.2018.10.034

858 [32] Engh IB. Molecular phylogeny of the *Cordyceps-Tolypocladium* complex. Candidate scientific
859 thesis, Department of Biology, University of Oslo. 1999.

860 [33] Zhao J, Wang N, Chen Y-Q, Li T-H, Qu L-H. Molecular identification for the asexual stage of
861 *Cordyceps sinensis*. Acta Sci. Nat. Univ. Sunyatseni. 1999;38(1): 122–123.

862 [34] Kinjo N, Zang M. Morphological and phylogenetic studies on *Cordyceps sinensis* distributed in
863 southwestern China. Mycoscience. 2001;42: 567–574.

864 [35] Chen Y-Q, Wang N, Li T-H, Zhang W-M. Determination of the anamorph of *Cordyceps sinensis*
865 inferred from the analysis of the ribosomal DNA internal transcribed spacers and 5.8S rDNA.
866 Biochem. Syst. Ecol. 2001;29: 597–607.

867 [36] Chen Y-Q, Hu B, Xu F, Zhang W-M, Zhou H, Qu L-H. Genetic variation of *Cordyceps sinensis*, a
868 fruit-body-producing entomopathegenic species from different geographical regions in China.
869 FEMS Microbiol. Lett. 2004;230: 153–158.

870 [37] Liu Z-Y, Yao Y-J, Liang Z-Q, Liu A-Y, Pegler DN, Chase M-W. Molecular evidence for the
871 anamorph-teleomorph connection in *Cordyceps sinensis*. Mycol. Res. 2001;105(7): 827–832.

872 [38] He S-Q, Jin X-L, Luo J-C, Wang C-M, Wang S-R. Morphological characteristics and submerged
873 culture medium screening of a strain of *Geomyces pannorum* isolation from *Cordyceps sinensis*.
874 Chin. J. Grassland. 2010;32(z1): 70–75. https://d.wanfangdata.com.cn/periodical/zgcd2010z1017

875 [39] He S-Q, Jin X-L, Luo J-C, Wang C-M. Morphological characteristics and submerged culture
876 medium screening of *Pseudogymnoascus roseus*. Microbiol. Chin. 2011;38(9): 1371−1376.

877 [40] Zhang Y-J, Sun B-D, Zhang S, Wàngmǔ, Liu X-Z, Gong W-F. Mycobiotal investigation of natural
878 *Ophiocordyceps sinensis* based on culture-dependent investigation. Mycosistema. 2010;29(4):
879 518–527.

880 [41] Xia F, Liu Y, Shen G-L, Guo L-X, Zhou X-W. Investigation and analysis of microbiological
881 communities in natural *Ophiocordyceps sinensis*. Can. J. Microbiol. 2015;61: 104–111.

882 [42] Yang J-Y, Tong X-X, He C-Y, Bai J, Wang F, Guo J-L. Comparison of endogenetic microbial
883 community diversity between wild *Cordyceps sinensis*, artificial *C. sinensis* and habitat soil. Chin.
884 J. Chin. Materia Medica. 2021;46(12): 3106–3115.

885 [43] Li X-Z, Li Y-L, Zhu J-S. *Differential expression of mating-type genes in Hirsutella sinensis and*
886 *natural Cordyceps sinensis*. Proc. 2021 Intl. Conf. Info. Technol. Biomed. Engineering, 2021. pp.
887 318−333. Available from https://conferences.computer.org/icitbepub/pdfs/ICITBE2021-

888 6JNtJiThlp10s9N5Sodvuy/009900a318/009900a318.pdf

889 [44] Wei X-L, Yin X-C, Guo Y-L, Shen N-Y, Wei, J.-C. Analyses of molecular systematics on
890 *Cordyceps sinensis* and its related taxa. Mycosystema. 2006;25(2): 192–202.

891 [45] Mo M-H, Chi S-Q, Zhang K-Q. Microcycle conidiation of *Cordyceps sinensis* and anamorph
892 isolation. Mycosystema 2001;20: 482−485.

893 [46] Liu Z-Y, Liang Z-Q, Liu A-Y. Investigation on microcycle conidiation of ascospores and
894 conidiogenous structures of anamorph of *Cordyceps sinensis*. Guizhou Agricult. Sci. 2003;31(1):
895 3–5.

896 [47] Xiao Y-Y, Chen C, Dong J-F, Li C-R, Fan M-Z. Morphological observation of ascospores of
897 *Ophiocordyceps sinensis* and its anamorph in growth process. J. Anhui Agricult. Univ. 2011;38(4):
898 587–591.

899 [48] Wang N, Chen Y-Q, Zhang W-M, Li T-H, Qu L-H. Molecular evidence indicating multiple origins
900 in the entomogenous *Cordyceps*. Acta Sci. Nat. Univ. Sunyatseni. 2000;39: 70−73.

901 [49] Li Z-Z, Huang B, Li C-R, Fan M-Z. Molecular evidence for anamorph determination of *Cordyceps*
902 *sinensis* (Berk.) Sacc. Mycosystema. 2000;9(1): 60–64.

903 [50] Wei J-C, Wei X-L, Zheng W-F, Guo W, Liu R-D. Species identification and component detection
904 of *Ophiocordyceps sinensis* cultivated by modern industry. Mycosystema. 2016;35(4): 404–410.

905 [51] Hu X, Zhang Y-J, Xiao G-H, Zheng P, Xia Y-L, Zhang X-Y, St Leger RJ, Liu X-Z, Wang C-S.
906 Genome survey uncovers the secrets of sex and lifestyle in caterpillar fungus. Chin. Sci. Bull.
907 2013;58: 2846–2854.

908 [52] Li Y, Hsiang T, Yang R-H, Hu X-D, Wang K, Wang W-J, et al. Comparison of different sequencing
909 and assembly strategies for a repeat-rich fungal genome, *Ophiocordyceps sinensis*. J. Microbiol.
910 Methods. 2016;128: 1−6.

911 [53] Liu J, Guo L-N, Li Z-W, Zhou Z, Li Z, Li Q, et al. Genomic analyses reveal evolutionary and
912 geologic context for the plateau fungus *Ophiocordyceps sinensis*. Clin. Med. 2020;15: 107–119.

913 [54] Jin L-Q, Xu Z-W, Zhang B, Yi M, Weng C-Y, Lin S, et al. Genome sequencing and analysis of
914 fungus *Hirsutella sinensis* isolated from *Ophiocordyceps sinensis*. AMB Expr. 2020;10: 105.
915 https://doi.org/10.1186/s13568-020-01039-x

916 [55] Shu R-H, Zhang J-H, Meng Q, Zhang H, Zhou G-L, Li M-M, et al. A new high-quality draft

917 genome assembly of the Chinese cordyceps *Ophiocordyceps sinensis*. Genome Biol. Evol.
918 2020;12(7): 1074−1079.

919 [56] Li X-Z, Li Y-L, Yao Y-S, Xie W-D, Zhu J-S. Further discussion with Li et al. (2013, 2019)
920 regarding the "ITS pseudogene hypothesis" for *Ophiocordyceps sinensis*. Mol. Phylogenet. Evol.
921 2020;146: 106728. https://doi.org/10.1016/j.ympev.2019.106728

922 [57] Zhang Y-J, Xu L-L, Zhang S, Liu X-Z, An Z-Q, Wàngmǔ, et al. Genetic diversity of
923 *Ophiocordyceps sinensis*, a medicinal fungus endemic to the Tibetan Plateau: implications for its
924 evolution and conservation. BMC Evol. Biol. 2009;9: 290. doi:10.1186/1471-2148-9-290

925 [58] Cheng Q-Q, Cheng C-S, Ouyang Y, Lao C-C, Cui H, Xian Y, et al. Discovery of differential
926 sequences for improving breeding and yield of cultivated *Ophiocordyceps sinensis* through ITS
927 sequencing and phylogenetic analysis. Chin. J. Nat. Med. 2018;16(10): 0749−0755.

928 [59] Mao X-M, Zhao S-M, Cao L, Yan X, Han R-C. The morphology observation of *Ophiocordyceps*
929 *sinensis* from different origins. J Environ. Entomol. 2013;35(3): 343–353.

930 [60] Chen C-S, Hseu R-S, Huang C-T. Quality control of *Cordyceps sinensis* teleomorph, anamorph,
931 and Its products. Chapter 12, *in* (Shoyama, Y., Ed.) *Quality Control of Herbal Medicines and*
932 *Related Areas*. InTech, Rijeka, Croatia, 2011. www.intechopen.com

933 [61] Li Y, Jiao L, Yao Y-J. Non-concerted ITS evolution in fungi, as revealed from the important
934 medicinal fungus *Ophiocordyceps sinensis*. Mol. Phylogenet. Evol. 2013;68: 373−379.

935 [62] Liang Z-Q. Anamorphs of *Cordyceps* and their determination. Southwest Chin. J. Agricult. Sci.
936 1991;4(4): 1–8.

937 [63] Tjedje JM, Asuming-Brempong S, Nüsslein K, Marsh TL, Flynn SJ. Opening the black box of soil
938 microbial diversity. Appl. Soil. Ecol. 1999;13: 109–122.

939 [64] Schmeisser C, Steele H, Streit W. Metagenomics，biotechnology with non-culturable microbes.
940 Appl. Microbiol. Biotechnol. 2007;75: 955–962.

941 [65] Stensrud Ø, Hywel-Jones NL, Schumacher T. Toward a phylogenetic classification of *Cordyceps*:
942 ITS nrDNA sequence data confirm divergent lineages and paraphyly. Mycol. Res. 2005;109:
943 41−56.

944 [66] Stensrud Ø, Schumacher T, Shalchian-Tabrizi K, Svegardenib IB, Kauserud H. Accelerated
945 nrDNA evolution and profound AT bias in the medicinal fungus *Cordyceps sinensis*. Mycol. Res.
946 2007;111: 409–415.

947 [67] Yang J-Y, Tong X-X, He C-Y, Bai J, Wang F, Guo J-L. Comparison of endogenetic microbial
948 community diversity between wild *Cordyceps sinensis*, artificial *C. sinensis* and habitat soil. Chin.
949 J. Chin. Materia Medica. 2021;46(12): 3106–3115.

950 [68] Li Y-L. Preliminary study on the ascospores of *Cordyceps sinensis*. Edible Fungi Chin.
951 2002;21(4): 9−10.

952 [69] Li Y-L, Li X-Z, Yao Y-S, Wu Z-M, Lou Z-Q, Xie W-D, et al. Altered GC- and AT-biased genotypes
953 of *Ophiocordyceps sinensis* in the stromal fertile portions and ascospores of natural *Cordyceps*
954 *sinensis*. PLOS ONE 2022. (Submitted as a companion paper)

955 [70] Lin W-C, Wu Y-W, Xie M-C, Zhu J-S. Reduced liver necrosis and fibrosis and improved liver
956 functions in a CCl4-induced hepatitis model by ReishiMax supplementation. Gastroenterol.
957 2004;126(4II): A431.

958 [71] Wang Y-B, Wang Y, Fan Q, Duan D-E, Zhang G-D, Dai R-Q, et al. Multigene phylogeny of the
959 family *Cordycipitaceae* (Hypocreales): new taxa and the new systematic position of the Chinese
960 cordycipitoid fungus *Paecilomyces hepiali*. Fungal Diversity 2020;103: 1–46.

961 [72] Chen J, Zhang W, Lu T. Morphological and genetic characterization of a cultivated *Cordyceps*
962 *sinensis* fungus and its polysaccharide component possessing antioxidant property in H22 tumor-
963 bearing mice. Life Sci. 2006;78(23): 2742−2748.

964 [73] Leung P-H, Zhang Q-X, Wu J-Y. Mycelium cultivation, chemical composition and antitumour
965 activity of a *Tolypocladium* sp. fungus isolated from wild *Cordyceps sinensis*. J. Appl. Microbiol.
966 2006;101(2): 275−283.

967 [74] Barseghyan GS, Holliday JC, Price TC, Madison LM, Wasser SP. Growth and cultural-
968 morphological characteristics of vegetative mycelia of medicinal caterpillar fungus
969 *Ophiocordyceps sinensis* G.H. Sung et al. (Ascomycetes) Isolates from Tibetan Plateau
970 (P.R.China). Intl. J. Med. Mushrooms. 2011;13(6): 565−581.

971 [75] Huelsenbeck JP, Ronquist F. MRBAYES: Bayesian inference of phylogeny. Bioinformat. 2001;17:
972 754−755.

973 [76] Bushley KE, Li Y, Wang W-J, Wang X-L, Jiao L, Spatafora JW, et al. Isolation of the MAT1-1
974 mating type idiomorph and evidence for selfing in the Chinese medicinal fungus *Ophiocordyceps*
975 *sinensis*. Fungal Biol. 2013;117(9): 599−610.

976 [77] Li Y-L, Yao Y-S, Zhang Z-H, Xu H-F, Liu X, Ma S-L, et al. Synergy of fungal complexes isolated
977 from the intestines of *Hepialus lagii* larvae in increasing infection potency. J. Fungal Res.
978 2016;14: 96−112.

979 [78] Zhang, S.; Zhang, Y.-J. Molecular evolution of three protein-coding genes in the Chinese
980 caterpillar fungus *Ophiocordyceps sinensis*. Microbiol. China. 2015;42(8): 1549−1560.

981 [79] Liu Z-Q, Lin S, Baker PJ, Wu L-F, Wang X-R, Wu H, Xu F, et al. Transcriptome sequencing and
982 analysis of the entomopathogenic fungus *Hirsutella sinensis* isolated from *Ophiocordyceps*
983 *sinensis*. BMC Genomics. 2015;16: 106–123.

984 [80] Pang F, Wang L-P, Jin Y, Guo L-P, Song L-P, Liu G-M, et al. Transcriptome analysis of
985 *Paecilomyces hepiali* at different growth stages and culture additives to reveal putative genes in
986 cordycepin biosynthesis. Genomics 2018;110: 162–170.

987 [81] Zhang S, Zhang Y-J, Shrestha B, Xu J-P, Wang C-S, et al. *Ophiocordyceps sinensis* and *Cordyceps*
988 *militaris*: research advances, issues and perspectives. Mycosystema. 2013;32: 577−597.

989 [82] Ma S-L, Zhang Z-H, Xu H-F, Liu X, Li Y-L. Analysis microorganism flora isolated from the
990 intestine of living larvae of *Hepialus lagii* Yan SP Nov. and inoculation studies. Edible Fungi.
991 2014;3: 28–30.

992 [83] Quandt CA, Kepler RM, Gams W, Araújo JPM, Ban S, Evans HC, et al. Phylogenetic-based
993 nomenclatural proposals for *Ophiocordycipitaceae* (Hypocreales) with new combinations in
994 *Tolypocladium*. IMA Fungus 2014;5: 121−134.